

Conformationally Constrained Analogues of Diacylglycerol (DAG). 28. DAG-dioxolanones Reveal a New Additional Interaction Site in the C1b Domain of PKC δ

Yongseok Choi,^{‡,§,¶} Yongmei Pu,^{§,#} Megan L. Peach,^{||,#} Ji-Hye Kang,[‡] Nancy E. Lewin,[§] Dina M. Sigano,[‡] Susan H. Garfield,[⊥] Peter M. Blumberg,^{*,§} and Victor E. Marquez^{*,‡}

Laboratory of Medicinal Chemistry, Center for Cancer Research, National Cancer Institute—Frederick, National Institutes of Health, Frederick, Maryland 21702, Laboratory of Cancer Biology and Genetics and Laboratory of Experimental Carcinogenesis, Center for Cancer Research, National Cancer Institute, National Institutes of Health, Bethesda, Maryland 20892, and Basic Research Program, SAIC-Frederick, Inc., NCI—Frederick, Frederick, Maryland 21702

Received March 7, 2007

Diacylglycerol (DAG) lactones have provided a powerful platform for structural exploration of the interactions between ligands and the C1 domains of protein kinase C (PKC). In this study, we report that DAG-dioxolanones, novel derivatives of DAG-lactones, exploit an additional point of contact (glutamine 27) in their binding with the C1b domain of PKC δ . Mutation of this point of contact to glutamate selectively impairs binding of the DAG-dioxolanones compared to that of the corresponding DAG-lactones (1200- to 3000-fold versus 35- to 55-fold, respectively). The differential response of this mutated C1b domain to the DAG-dioxolanones relative to the DAG-lactones provides a unique tool to probe the role of the C1b domain in PKC δ function, where the response to the DAG-lactones affords a positive control for retained function. Using this approach, we show that the C1b domain of PKC δ plays the predominant role in the translocation of PKC δ to the membrane in the presence of DAG.

Introduction

The lipophilic second messenger diacylglycerol (DAG^a), produced through hydrolysis of phosphatidylinositol 4,5-bisphosphate (PIP₂) by the activation of receptor-coupled phospholipase C (PLC) or indirectly from phosphatidylcholine via phospholipase D,¹ plays a central role in signal transduction of numerous physiological and pathological events including proliferation, differentiation, apoptosis, angiogenesis, and drug resistance.^{2–6} These diverse functions of the DAG signal are realized through binding with high affinity to a class of zinc finger structures, the so-called “C1 domains”. C1 domains were first identified in PKC as the interaction site for DAG and phorbol esters.⁷ It is now recognized, however, that PKC is only

one of multiple families of proteins that have appropriate C1 domains to act as DAG receptors.⁸ The other DAG responsive families include the PKD family,⁹ a distinct class of serine/threonine kinases; the chimaerin family,¹⁰ inhibitors of p21Rac; the munc-13 family,¹¹ proteins involved in synaptic vesicle priming; the RasGRP family,^{12,13} guanyl nucleotide exchange factors for Ras and Rap1; and the DAG kinase family,^{14,15} which functions to abrogate DAG signaling, thus providing negative feedback on DAG signaling pathways. Of these C1 domain-containing families, the PKC family is the best-studied mediator in the DAG signaling pathway and an important target for drug development.

The PKC family of serine/threonine kinases consists of 10 members that are divided into three classes: (i) the classical PKCs (cPKCs α , β I, β II, γ); (ii) the novel PKCs (nPKCs δ , ϵ , η , θ); the atypical PKCs (aPKCs ζ , ι/λ). Both the classic and novel PKCs contain two tandem C1 domains (C1a and C1b) in their N-terminal regulatory region that bind to DAG in a Ca²⁺-dependent (cPKCs) or -independent manner (nPKCs). Besides C1 domains, the regulatory region of the cPKCs and nPKCs also contains a pseudosubstrate domain, which can interact with the catalytic site of the C-terminal kinase domain to inhibit the kinase activity. Binding of DAG to the C1 domain completes a hydrophobic surface on the C1 domain, favoring its interaction with the membrane and causing the membrane translocation of the whole PKC protein.¹⁶ This DAG-C1 domain–membrane interaction is coupled to a conformational change in PKC, causing the release of the pseudosubstrate domain from the catalytic site and thereby activating the enzyme.⁸

Multiple classes of high-affinity ligands for the C1 domains of PKCs have been described. These ligands include the diterpenes such as the phorbol esters, macrocyclic lactones such as the bryostatins, polyacetates such as aplysiatoxin, or indole alkaloids such as teleocidin.¹⁷ Unfortunately, with the exception of the indole alkaloids, the complicated structures of these ligands have largely prevented their further development through medicinal chemistry. Taking advantage of the DAG derivatives,

* To whom correspondence should be addressed. For P.M.B.: phone, 301-496-3189; fax, 301-496-8709; e-mail, blumberp@dc37a.nci.nih.gov. For V.E.M.: phone, 301-846-5954; fax, 301-846-6033; e-mail, marquezv@mail.nih.gov.

[‡] National Cancer Institute—Frederick.

[‡] Current address: Laboratory of Molecular Therapeutics, School of Biosciences and Biotechnology, Korea University, Anam-dong Seongbuk-gu, Seoul 136-701, Korea. E-mail: ychoi@korea.ac.kr.

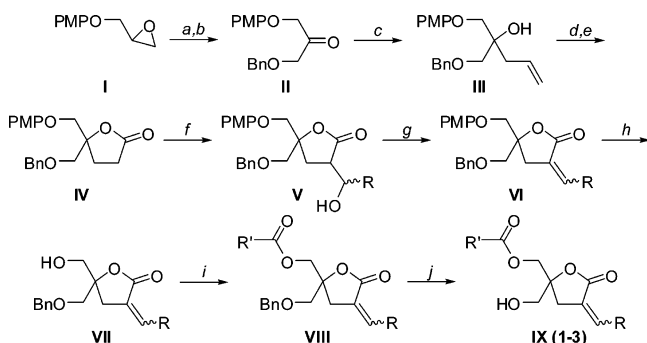
[#] These authors contributed equally to this work.

[§] Laboratory of Cancer Biology and Genetics, National Cancer Institute.

^{||} SAIC-Frederick, Inc.

[⊥] Laboratory of Experimental Carcinogenesis, National Cancer Institute.

^a Abbreviations: CAN, ceric ammonium nitrate; CHO, Chinese hamster ovary; DAG, diacylglycerol; DBU, 1,8-diazabicyclo[5.4.0]undec-7-ene; DMAP, dimethylaminopyridine; DMS, dimethyl sulfide; DNA, deoxyribonucleic acid; FABMS, fast atom bombardment mass spectra; GFP, green fluorescent protein; GST, glutathione S-transferase; HAART, highly active antiretroviral therapy; HIV/AIDS, human immunodeficiency virus/acquired immune deficiency syndrome; IL-6, interleukin 6; IPTG, isopropyl-*O*-D-thiogalactopyranoside; LB, Luria broth; LDA, lithium diisopropylamide; LiHMDS, lithium hexamethyldisilylazide; MsCl, methanesulfonyl chloride; NMR, nuclear magnetic resonance; OD, optical density; PCC, pyridinium chlorochromate; PCR, Polymerase chain reaction; PDBu, phorbol 12,13-dibutyrate; PIP₂, phosphatidylinositol 4,5-bisphosphate; PKC, protein kinase C; PKD, protein kinase D; PLC, phospholipase C; PMA, phorbol 12-myristate-13-acetate; PMP, *p*-methoxyphenyl; pTosOH, *p*-toluenesulfonic acid; SDS–PAGE, sodium dodecyl sulfate polyacrylamide gel electrophoresis; SEM, standard error of the mean; THF, tetrahydrofuran; TLC, thin layer chromatography.

Scheme 1^a

^a (a) NaH, BnOH, Δ ; (b) PCC, 4 Å molecular sieves, CH_2Cl_2 ; (c) allylmagnesium bromide, THF, -78°C ; (d) $\text{BH}_3\cdot\text{SMe}_2$, THF, -78°C ; (e) PCC, CH_2Cl_2 ; (f) LiHMDS, RCHO, THF, -78°C ; (g) (i) Et_3N , MsCl, CH_2Cl_2 , $0^\circ\text{C} \rightarrow \text{room temp}$; (ii) DBU; (h) CAN, CH_3CN , H_2O , 0°C ; (i) Et_3N , DMAP, $\text{R}'\text{C}(\text{O})\text{Cl}$, CH_2Cl_2 , $0^\circ\text{C} \rightarrow \text{room temp}$; (j) BCl_3 , CH_2Cl_2 , -78°C .

in which the flexibility of the structure has been constrained to reduce the entropic loss due to binding,¹⁷ our group has developed a series of DAG-lactones with K_i values for binding to PKC approaching those of phorbol esters.¹⁷ These structures have provided promising lead compounds for selective actions mediated by subsets of the DAG-responsive proteins.^{18,19} They likewise have proven to be powerful tools for probing the detailed molecular interactions underlying ligand binding to the C1 domains.¹⁷

In this study, we describe the characterization of dioxolanone analogues of the DAG-lactones. These compounds were predicted by molecular modeling to incorporate an additional site of interaction within the binding cleft of the C1 domain. Consistent with this prediction, we show that these compounds are orders of magnitude more sensitive to disruption of this predicted site of interaction through mutation of the C1 domain.

Chemistry

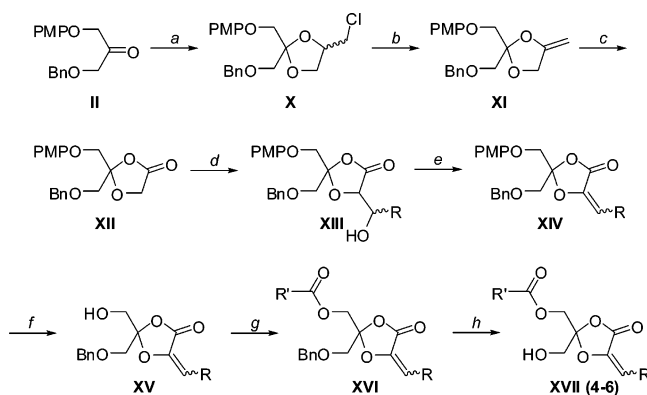
As illustrated in Scheme 1, target DAG-lactones (**1–3**, Table 1) were synthesized in racemic form starting from commercially available glycidyl-4-methoxyphenyl ether, according to methodology previously developed in our laboratory.^{20–22} As before, the DAG-lactones were successfully separated into both *E*- and *Z*-isomers. The vinyl proton of the *Z*-isomers displayed a characteristic multiplet at δ 6.20–6.24, while the corresponding signal for the *E*-isomer appeared more downfield at δ 6.72–6.78. The final target DAG-lactones appear in Table 1.

Our strategy for assembling the functionalized DAG-dioxolanone targets focused on constructing a central 1,3-dioxolan-4-one skeleton (**XII**) that could be elaborated in a manner similar to the DAG-lactones (Scheme 2). Accordingly, reaction of common intermediate **II** with commercially available 3-chloro-1,2-propanediol under acidic conditions gave **X**. Base-catalyzed elimination, followed by ozonolysis of the resultant double bond gave **XII**, the dioxolanone equivalent to DAG-lactone **IV**. Aldol-type condensation of **XII** with either 3-isobutyl-5-methylhexanal or isovaleryl aldehyde gave **XIII**, which was not purified but immediately subjected to elimination conditions to give **XIV**. Deprotection of the PMP group followed by acylation led to **XVI**, and upon debenzoylation, the desired racemic 1,3-dioxolan-4-one analogues (**XVII**, **4–6**) were obtained. In the case of the DAG-dioxolanones, all the final compounds were obtained as inseparable mixtures of *E*- and *Z*-isomers except for **5**, which was obtained as a single isomer whose geometric stereochemistry could not be determined. The final target DAG-dioxolanones appear in Table 1.

Table 1. Inhibitory Dissociation Constants (K_i) of DAG-lactones and Corresponding DAG-dioxolanones for PKC α ^a

DAG-lactone (log <i>P</i> = 4.27)	K_i (nM)	DAG-dioxolanones (log <i>P</i> = 3.82)	K_i (nM)
Z-1 ²⁴	2.90 ± 0.35	E,Z-4 ^b	6.41 ± 0.76
Z-2	3.49 ± 0.57	5 ^c	19.83 ± 0.52
Z-3	3.07 ± 0.40	E,Z-6 ^b	5.78 ± 0.95

^a The K_i values were measured by competitive binding of the compounds for the receptor against [³H]PDBu. Each value is an average of three independent experiments, expressed as the mean ± SEM. The partition coefficients (log *P*) were calculated according to the atom-based program MOE SLog *P*.²³ ^b Mixture of *E* and *Z* isomers. ^c Single geometric isomer (*E* or *Z*).

Scheme 2^a

^a (a) 3-Chloro-1,2-propanediol, pTsOH·H₂O, C₆H₆, Δ ; (b) KO^tBu, THF, Δ ; (c) (i) O₃, MeOH/ CH_2Cl_2 , -78°C ; (ii) DMS, room temp; (d) (i) LiHMDS, THF, -78°C ; (ii) RCHO; (e) (i) Et_3N , MsCl, CH_2Cl_2 , $0^\circ\text{C} \rightarrow \text{room temp}$; (ii) DBU; (f) CAN, CH_3CN , H_2O ; (g) Et_3N , DMAP, $\text{R}'\text{C}(\text{O})\text{Cl}$, CH_2Cl_2 , $0^\circ\text{C} \rightarrow \text{room temp}$; (h) BCl_3 , CH_2Cl_2 , -78°C .

Results

Binding Potencies of the DAG-dioxolanones Were Maintained at the Level of Their Corresponding DAG-lactones.

The potencies of the three DAG-dioxolanones prepared were first evaluated for binding to PKC α , which has been our routine assay for the DAG-lactones. The binding affinities of the parent DAG-lactones were measured for comparison, and for simplicity only the data for the *Z*-isomers are included (Table 1). The differences in potencies between *Z*- and *E*-isomers for DAG-lactones are small and vary from 1.1- to 1.8-fold, generally in favor of the *Z*-isomer. All the DAG-dioxolanones were potent ligands, with K_i values 2- to 6-fold weaker than those of their corresponding DAG-lactones. These results indicate that the introduction of the oxygen in the ring system to form the dioxolanone ring was well tolerated. However, the anticipated formation of an additional hydrogen bond did not lead to an overall enhancement in binding, implying that the additional

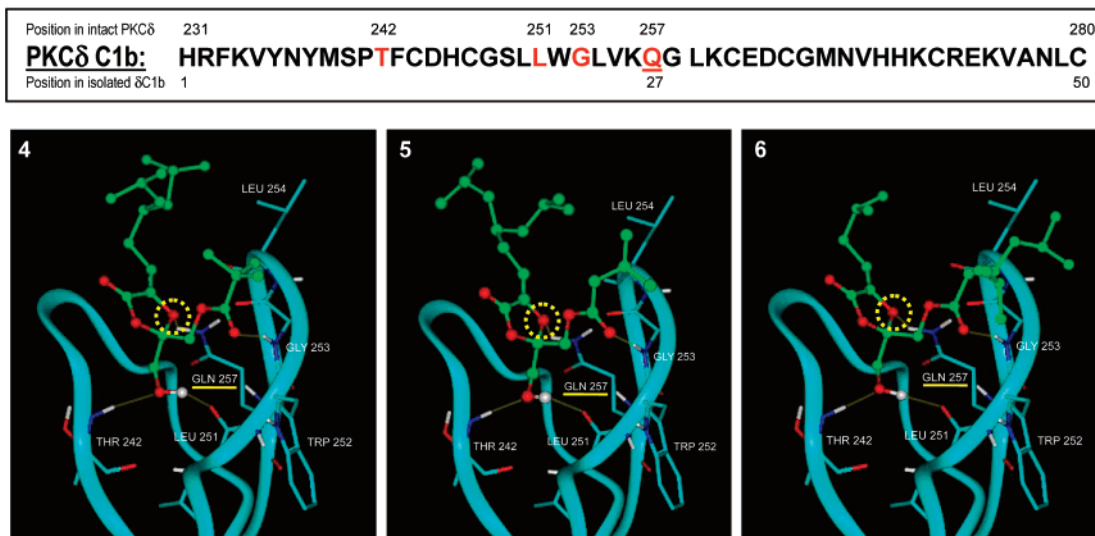


Figure 1. Docking prediction of interactions between C1b domain of PKC δ and DAG-dioxolanones 4–6 (Z-isomers). The amino acid sequence of the C1b domain of PKC δ is shown in the upper panel. The residues that form hydrogen bonds with the DAG-dioxolanones are marked in red. The added oxygen in the ring structure forms a new hydrogen bond with the glutamine residue (GLN 257), as shown in the yellow circles. The indicated glutamine residue is underlined both in the upper panel and in the lower pictures. The DAG-dioxolanone structure is shown in green.

binding energy of this hydrogen bond was counterbalanced by a poorer overall fit into the C1 domain (vide infra).

Prediction from Computer Modeling of an Additional Site of Interaction in the PKC δ C1b Domain upon Conversion of the DAG-lactone to the Corresponding DAG-dioxolanone.

DAG-lactones have provided a powerful platform for probing the interactions of ligands with the C1 domains. Our modeling studies of these binary complexes have identified two alternative binding modes, designated as *sn*-1 or *sn*-2, depending on the identity of the carbonyl engaged in binding to the protein. The *sn*-1 binding mode is defined as that in which the *sn*-1 carbonyl is hydrogen-bonded to the C1 domain, and for the alternative *sn*-2 binding mode, it is the *sn*-2 carbonyl that appears directly engaged in hydrogen bonding to the protein. Although from the modeling perspective both binding modes appear to form an identical network of hydrogen bonds as was observed with phorbol 13-*O*-acetate, we have determined that DAG-lactones bind preferentially in the *sn*-2 binding mode.^{25,26} This binding mode is additionally enhanced by the presence of highly branched α -alkylidene side chains, which lie adjacent to the *sn*-2 carbonyl. In such binding mode the orphan *sn*-1 carbonyl binds at the membrane interface.^{25,26}

We performed computational docking studies to predict the binding mode and the interactions formed between the PKC δ C1b domain and the new DAG-dioxolanone compounds. The computer modeling demonstrated that the added oxygen could form an additional hydrogen bond in the binding cleft of the δ C1b domain with the side chain of the glutamine residue at position 257 (numbered as position 27 in the isolated δ C1b domain) *only* in the less favorable *sn*-1 binding mode. This glutamine residue, although important for the structural integrity of the C1 domain,²⁷ is not predicted to interact with the DAG-lactones directly. In the *sn*-1 binding mode, four amino acids are predicted to form hydrogen bonds with the DAG-dioxolanones (marked in red in the upper panel of Figure 1). Thr242, Leu251, and Gly253 form three hydrogen bonds with the hydroxyl group and the *sn*-1 carbonyl group respectively on the side chain of the DAG-lactone backbone. The added oxygen in the ring system (marked with a yellow dashed circle in each image in Figure 1) forms the fourth hydrogen bond with the Gln257 residue (underlined in the figure). As discussed in the previous section, this additional hydrogen bond did not lead to

Table 2. Inhibitory Dissociation Constants (K_i) of the Dioxolanones (4–6) and Their Corresponding DAG Lactones (Z-1, Z-2, Z-3) from the Wild-Type C1b Domain of PKC δ (wt δ C1b) and the Glutamate Mutant (Q27E)^a

	$K_{wt/\delta C1b}$ (nM)	$K_{Q27E/\delta C1b}$ (nM)	$K_{Q27E/\delta C1b}/K_{wt/\delta C1b}$
4 ^b	0.82 \pm 0.07	2510 \pm 220	3070
Z-1 ^c	1.15 \pm 0.07	44.8 \pm 4.5	39
5 ^b	2.82 \pm 0.36	3460 \pm 210	1230
Z-2 ^c	0.96 \pm 0.09	53.0 \pm 3.7	55
6 ^b	0.90 \pm 0.07	1720 \pm 160	1910
Z-3 ^c	2.13 \pm 0.15	73.72 \pm 5.3	35
PDBu	0.33 \pm 0.05	6.2 \pm 1.0	19

^a The K_i values were measured by competitive binding of the compounds for the receptors against [³H]PDBu. Each value is an average of three independent experiments, expressed as the mean \pm SEM. Ratios of K values (third column) of Mutant to K values of wild type (K_i for DAG-lactones and DAG-dioxolanones; K_d for PDBu) indicate the change in potency. ^b DAG-dioxolanones. ^c DAG-lactones.

an overall enhancement in binding because it was counterbalanced by the poorer *sn*-1 binding mode involving the conformationally flexible *sn*-1 carbonyl rather than the conformationally rigid lactone carbonyl, thus voiding the entropic advantage of the *sn*-2 binding mode.

The Glutamine Residue of the Isolated δ C1b Plays an Important Role in Binding by the DAG-dioxolanones but Not by the Corresponding DAG-lactones. To verify the role of Gln257 in the interaction with the DAG-dioxolanones, we used site-directed mutagenesis to convert the glutamine (Gln) to glutamate (Glu). For ease of analysis, we performed the site directed mutagenesis on the isolated C1b domain of PKC δ (where the glutamine is in position 27 relative to the start of the C1b domain, with the mutant thus designated Q27E). The C1b mutant (Q27E/ δ C1b) was expressed and purified as a GST-fusion protein from *E. coli*. Scatchard analysis was performed to determine the dissociation constant (K_d) of the Q27E/ δ C1b mutant for binding to [³H]PDBu. The K_d value we obtained was 6.2 \pm 1.0 nM (three experiments, mean \pm SEM). Compared with the K_d of the wild-type δ C1b for PDBu (0.33 \pm 0.05 nM, three experiments, mean \pm SEM), the binding potency of the Q27E/ δ C1b mutant was decreased about 20-fold (Table 2). Such an effect on binding of [³H]PDBu was not unexpected, given the important role of this residue in the overall folding of the C1 domain.²⁷ Although this residue has been predicted not to

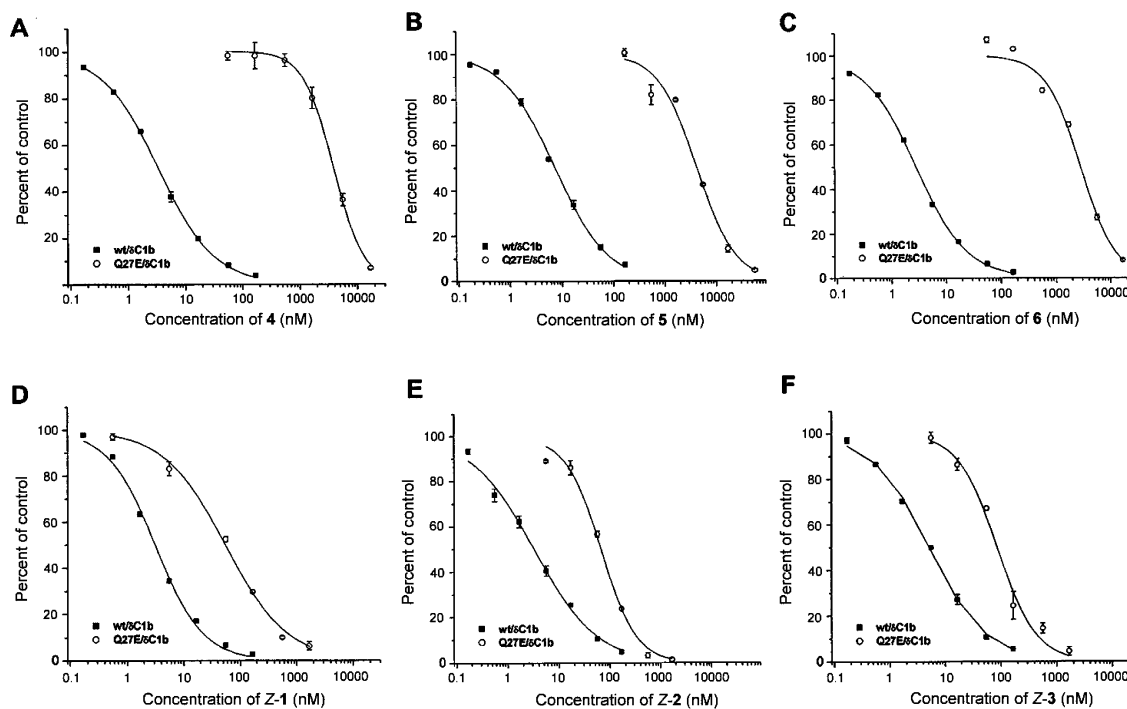


Figure 2. Dose response curves of the DAG-dioxolanones (A–C) and their corresponding DAG lactones (D–F) for binding to isolated wild-type C1b domain (wt/ δ C1b) and the C1b mutant (Q27E/ δ C1b) of PKC δ . The curves were obtained from the competitive binding of these compounds in the presence of [3 H]PDBu. Each curve is from a single experiment. All experiments were performed at least two additional times, with similar results: (A, D) dose response curves for the DAG-dioxolanone **4** and its corresponding DAG-lactone Z-1; (B, E) dose response curves for DAG-dioxolanone **5** and its corresponding DAG-lactone Z-2; (C, F) dose response curves for DAG-dioxolanone **6** and its corresponding DAG-lactone Z-3.

interact with phorbol esters directly, it forms bridging hydrogen bonds at the point where the large β sheet of C1b comes apart at one end of the binding groove.¹⁶ However, by the replacement with a very similar amino acid, glutamate, the folding could evidently be maintained for binding to PDBu with an affinity in the 10^{-9} M range. For comparison, all binding activity for PDBu was lost upon mutation of Gln27 to Gly or Trp, and binding affinities were reduced to 22 or 105 nM upon mutation to Val or Thr, respectively.²⁷

The K_i values of the DAG-dioxolanones **4–6** for the Q27E/ δ C1b mutant were measured and compared with those for the wild-type δ C1b domain. Dramatic differences were observed between the wild-type δ C1b and the Q27E/ δ C1b mutant in the binding to the DAG-dioxolanones. All the DAG-dioxolanones bound to the Q27E/ δ C1b mutant with a much weaker binding affinity compared with the wild type (Figure 2A–C). For example, **4** bound to the wild-type C1b with a K_i of 0.82 ± 0.07 nM (three experiments, mean \pm SEM), whereas for the mutant the K_i was 2510 ± 220 nM (three experiments, mean \pm SEM) (Figure 2A, Table 2), corresponding to a 3000-fold decrease in binding potency. The other two DAG-dioxolanones **5** and **6** (Figure 2B,C; Table 2) behaved similarly.

In contrast to the dramatic decreases in binding potencies of the DAG-dioxolanones to the Q27E/ δ C1b mutant, the binding affinities of the corresponding DAG lactones Z-1, Z-2, and Z-3 showed much more modest decreases of 35- to 55-fold, similar to the 20-fold decrease in potency for PDBu (Figure 2D–F, Table 2). Our results support the prediction from the molecular modeling that the Gln will provide a unique interaction with the ring oxygen of the dioxolanone. They are likewise consistent with the prediction from the studies with the wild-type C1 domain, that the lack of enhanced potency in the presence of the additional hydrogen bond to the Gln implies that in its

absence the DAG-dioxolanones would bind correspondingly more weakly in the *sn*-1 binding mode.

Does the Glutamine Residue (Q27) in the Isolated δ C1a Domain Play a Similar Role in the DAG-dioxolanone Interaction? Glutamine residue Q27 is highly conserved among different C1 domains including the C1a and C1b domains of PKC δ (see Figure 4A), but it is becoming increasingly clear that different C1 domains show substantial differences in their interactions with ligands.^{19,28} Does the dioxolanone ring also form a new interaction with the δ C1a domain through the glutamine residue at the indicated position? To answer this question, we mutated the glutamine residue at position 27 of the isolated δ C1a domain into glutamate as had been done for the δ C1b domain. Then we examined the binding affinity of the C1a mutant (Q27E/ δ C1a) for the DAG-dioxolanone **4**. The result was clearly different from what we observed with the Q27E/ δ C1b mutant. First, the binding affinity of the Q27E/ δ C1a mutant for PDBu was greatly reduced. The wild-type δ C1a potently bound PDBu with a K_d of 2.04 ± 0.24 nM (Table 3). However, after mutation, the K_d increased to 383 ± 15 nM for a 200-fold decrease of the binding potency. Compared to the C1b mutant (Q27E/ δ C1b) ($K_d = 6.2 \pm 1.0$ nM, Table 2), the δ C1a mutation (Q27E/ δ C1a) had a much greater effect on the phorbol ester binding, suggesting that the glutamine residue (Q27) plays a much more critical role in the protein folding of δ C1a. Second, the binding affinities of the Q27E/ δ C1a mutant for the DAG-dioxolanone and the corresponding DAG lactone were decreased to a similar degree. As shown in Table 3, both the DAG-dioxolanone **4** and the DAG-lactone Z-1 bound the wild-type δ C1a with high potency (K_i values of 4.31 ± 0.13 and 1.21 ± 0.11 nM, respectively). However, after mutation, the K_i values increased to 1567 ± 58 and 476 ± 6 nM, respectively. There were 390- and 360-fold decreases of the

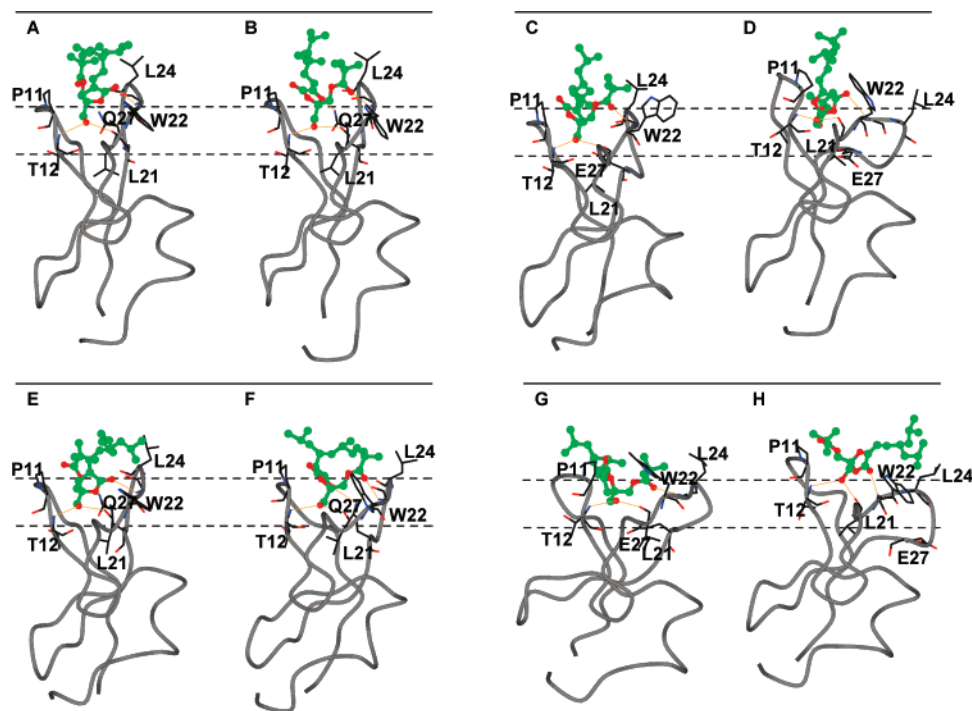


Figure 3. Representative structures from molecular dynamics simulations of C1 domains in the membrane environment. The center of the bilayer is indicated by a solid line, and the interfacial region is located between the two dashed lines. Hydrogen bonds to the ligands are indicated by gold-colored lines: (A) DAG-lactone Z-1 bound *sn*-2 to PKC δ C1b; (B) DAG-dioxolanone Z-4 bound *sn*-1 to PKC δ C1b; (C) DAG-lactone Z-1 bound *sn*-1 to Q27E/PKC δ C1b; (D) DAG-dioxolanone Z-4 bound *sn*-2 to Q27E/PKC δ C1b; (E) DAG-lactone Z-1 bound *sn*-2 to PKC δ C1a; (F) DAG-dioxolanone Z-4 bound *sn*-1 to PKC δ C1a; (G) DAG-lactone Z-1 bound *sn*-1 to Q27E/PKC δ C1a; (H) DAG-dioxolanone Z-4 bound *sn*-2 to Q27E/PKC δ C1a.

binding potencies of the DAG-dioxolanone and the corresponding DAG-lactone, respectively, for the Q27E/ δ C1a mutant. The approximately equal loss of the binding potency for PDBu, the DAG lactone, and the DAG-dioxolanone implies that the glutamine residue (Q27) in the δ C1a domain has a greater effect on the domain structure and function than the corresponding mutation in the δ C1b domain, since it abrogates binding with all ligands and not just the DAG-dioxolanones which form specific interactions with residue Q27.

Modeling the Dynamic Behavior of C1 Domains in the Membrane Environment. The sequences of PKC δ C1b and C1a are 42% identical, and the zinc-binding residues and residues essential for ligand binding are completely conserved. This suggests that the backbone structures of these two C1 domains are very similar. An examination of the static structure of δ C1b compared to a homology model of δ C1a does not offer any insight of why mutation of Q27 in these two domains has such widely different effects on ligand binding. To address this issue, we performed molecular dynamics simulations of DAG-lactone Z-1 and the corresponding DAG-dioxolanone 4 (Z-configuration) bound in the *sn*-1 and *sn*-2 orientations to the PKC δ C1a and C1b, Q27E/ δ C1a, and Q27E/ δ C1b domains. We have shown previously²⁵ that interactions between the C1 domain, its ligands, and the membrane environment are essential to understanding the structure and function of PKC. To take this into account, the simulations used an implicit solvent model that approximates the solvation effects of a lipid bilayer membrane, including the heterogeneous dielectric environment of the membrane interfacial region where water interacts with the lipid headgroups and glycerol backbones.²⁹

A starting configuration for each system was generated by translating and rotating the C1 domains to a position as hypothesized,¹⁶ with the top part of the C1 domain near the binding site inserted partially into the membrane. Each system

then underwent molecular dynamics simulation for 10 ns, over the course of which an ensemble of 100 snapshots of its structure was collected. We then calculated the average hydrogen-bonding interaction energy between the C1 domain and the DAG-lactone or DAG-dioxolanone for each ensemble (Table 4).

In both the wild-type δ C1b and δ C1a domains, DAG-lactones bind more strongly in the *sn*-2 orientation but DAG-dioxolanones prefer to bind *sn*-1. This is consistent with our earlier results from simulated annealing simulations in vacuum²⁶ and our predictions from the docking studies suggesting that the DAG-dioxolanones can form an extra hydrogen bond to the C1 domain in the *sn*-1 binding mode. With the mutant Q27E/ δ C1b and Q27E/ δ C1a domains, however, the situation is exactly reversed: DAG-lactones prefer the *sn*-1 binding mode, and DAG-dioxolanones prefer to bind *sn*-2. In the DAG-lactones, although they do not form a stable hydrogen bond with Gln27, the *sn*-2 binding mode is favored in part because of transient weak interactions between atom N ϵ of Gln27 and the *sn*-1 ester oxygen atoms. These become unfavorable repulsive interactions when Gln27 is mutated to Glu and the side chain nitrogen is replaced by an oxygen, so the *sn*-1 binding mode in which no polar atoms in the ligand are close to Glu27 is now preferred. With the DAG-dioxolanones, the hydrogen bond at the close contact between the extra ring oxygen and atom N ϵ of Gln27 becomes a heavy liability when Gln27 is mutated to Glu, and the *sn*-2 binding mode is an improvement, although here as with the DAG-lactones, there will still be unfavorable interactions with Glu27 and the *sn*-1 ester oxygens.

Representative structures from each simulation, with ligands in their favored binding modes, are shown in Figure 3. In all cases the C1 domains remain close to their starting configuration with the binding site loops buried in the interfacial region on one side of the membrane. The wild-type δ C1b domain (Figure 3A,B) retains its crystal conformation, and the ligand remains

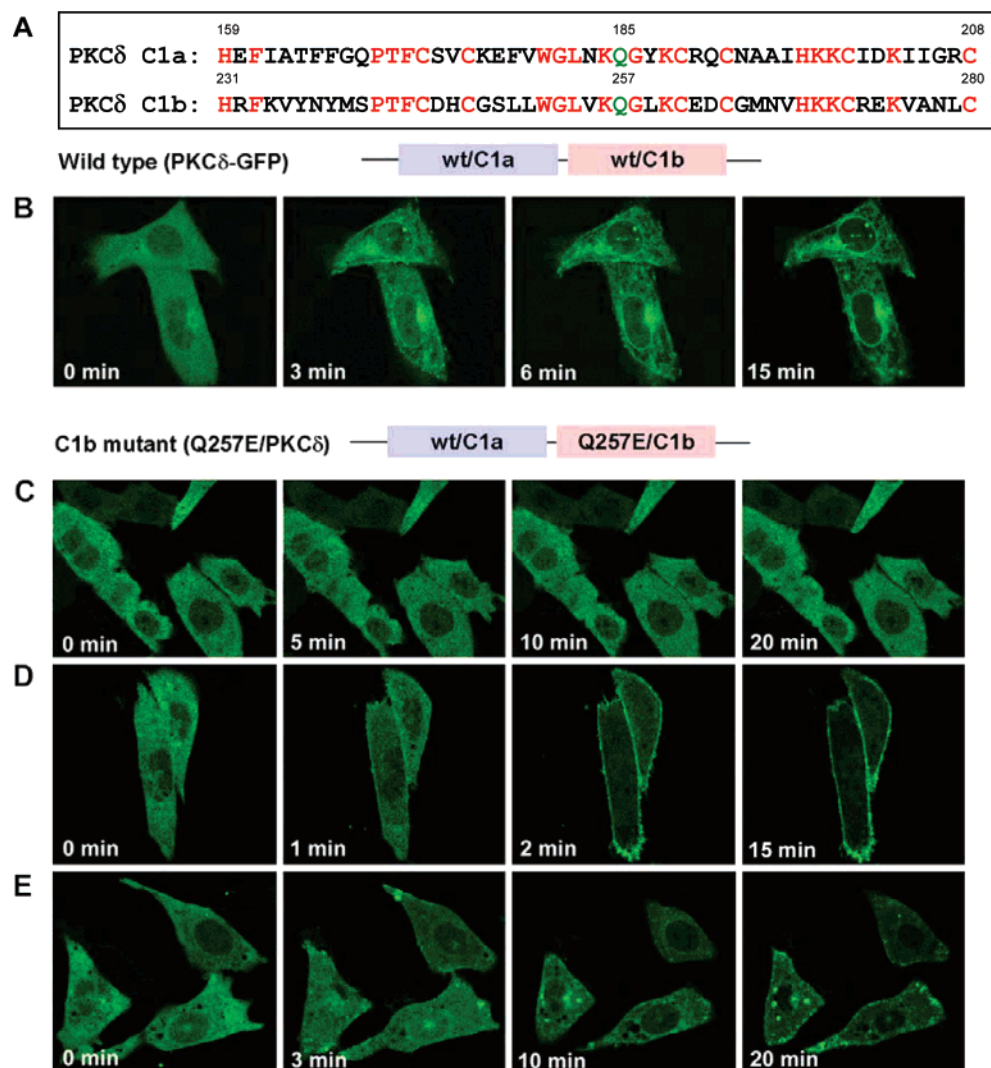


Figure 4. Confocal microscopy comparing membrane translocation of the wild-type full length PKC δ -GFP and its C1b mutant (Q257E/PKC δ -GFP) by the dioxolanone **4** in living CHO-K1 cells: (A) amino acid sequence alignment of the C1a and C1b domains of PKC δ , where the indicated glutamine residue is shown in green; (B) time serial images showing the dynamic translocation of wild-type PKC δ -GFP to the plasma membrane and internal membranes in living CHO-K1 cells after the application of **4** (20 μ M); (C) time serial images showing the distribution of the C1b mutant of PKC δ -GFP (Q257E) after the application of **4** (20 μ M), with no membrane translocation observed; (D) time serial images showing the dynamic translocation of the C1b mutant (Q257E) after the application of PMA (1 μ M); (E) time serial images showing the dynamic translocation of the C1b mutant (Q257E) after the application of Z-1 (20 μ M), the DAG-lactone corresponding to **4**. The minutes in each panel represent the time of drug treatment. Each experiment was performed at least three times with similar results.

Table 3. Comparison of the Binding Affinities of the DAG Dioxolanone **4**, the DAG-lactone Z-1 and PDBu for the Wild-Type C1a Domain of PKC δ (wt/ δ C1a), and the Glutamate Mutant (Q27E/ δ C1a)^a

	K_d (nM)	K_i (nM)	
		DAG-lactone Z-1	DAG-dioxolanone 4
phorbol ester			
PDBu			
Q27E/ δ C1a	383 \pm 15	476 \pm 6	1567 \pm 58
wt/ δ C1a	2.04 \pm 0.24	1.21 \pm 0.11	4.31 \pm 0.13
K_{Q27E}/K_{wt}	188	393	364

^a The K_i values were measured by competitive binding of the compounds for the receptors against [³H]PDBu. Each value is an average of three independent experiments, expressed as the mean \pm SEM.

stably bound. The wild-type δ C1a domain structure is also stable (Figure 3 E,F), although the binding site is opened about 1 Å wider as measured from tip to tip across the top, and it does not penetrate as far into the membrane as the δ C1b domain. This may explain why the δ C1a domain ligand binding affinity is generally slightly lower (Table 2, 3) and why it has different membrane translocating abilities than the δ C1b domain (vide

Table 4. Hydrogen-Bonding Interaction Energies (kcal/mol) between PKC δ C1 Domains and DAG Ligands.

	δ C1b	δ C1a	Q27E/ δ C1b	Q27E/ δ C1a
DAG-lactone Z-1	-103.18	-99.09	-104.28	-109.89
bound <i>sn</i> -1				
DAG-lactone Z-1	-106.68	-109.81	-100.41	-76.76
bound <i>sn</i> -2				
DAG-dioxolanone Z-4	-112.54	-109.48	-104.52	-101.03
bound <i>sn</i> -1				
DAG-dioxolanone Z-4	-109.62	-105.38	-124.21	-102.18
bound <i>sn</i> -2				

infra). A similar structure with a slightly opened binding site is observed with the mutant Q27E/ δ C1b domain bound to DAG-lactone (Figure 3C), although here the second binding site loop (residues 20–25) changes shape somewhat to allow residue Glu27 to be fully solvated outside the interfacial region. With the remaining mutant structures (Figure 3D,G,H), the binding site is severely distorted, with the second loop folded open to lie nearly horizontal to the plane of the bilayer. The binding site is a full 6 Å wider than in the δ C1b domain crystal structure.

These changes explain why the Q27E/ δ C1b domain has lost the ability to bind DAG-dioxolanones, and the Q27E/ δ C1a domain has lost all ligand binding ability. The changes in structure are driven by the necessity of solvating the mutant Glu27 residue, which is pulled out of the interfacial region of the bilayer by repulsive interactions between Glu27 and oxygen atoms in the DAG-dioxolanones and, in the case of the δ C1a domain, a lower membrane affinity in general.

Roles of the Individual C1 Domains in Membrane Translocation of Intact PKC δ in Response to DAG-dioxolanone Treatment in Living CHO Cells. (a) Mutating the Glutamine Residue (Q257) in the C1b Domain of Full-Length PKC δ Prevented Its Membrane Translocation in Response to DAG-dioxolanone Treatment. The dramatic effect of the Q27E mutation on the binding to the C1b domain of the DAG-dioxolanones, with a much more modest effect on the binding by phorbol esters or the DAG-lactones, now provides us with a powerful tool for probing the role of this domain in PKC δ function. Previously, an important role for the C1b domain had been indicated by using a P11G mutation, which dramatically reduces PDBu binding affinity.^{27,30} An underlying problem with interpretation, however, is that the overall effects of this mutation on PKC conformation cannot be assessed. In contrast, with the Q27E mutation in the C1b domain of PKC δ , a positive control is provided by PDBu or by the DAG-lactone, which still retains an adequate level of affinity, whereas binding to the DAG-dioxolanone should be lost.

We first studied the role of the C1b domain in PKC δ membrane translocation. We mutated the glutamine residue (Q257) of C1b in PKC δ -GFP to generate a C1b mutant of PKC δ (Q257E/PKC δ -GFP). Then, we monitored the response of the Q257E/PKC δ -GFP mutant to DAG-dioxolanone **4** in living CHO cells using real time confocal microscopy and compared this response to that to phorbol ester or a DAG-lactone. As shown in Figure 4B, **4** (20 μ M) translocated the wild-type PKC δ -GFP to both the plasma membrane and the internal membranes within 5 min after DAG-dioxolanone administration. However, no membrane translocation was observed in the C1b mutant (Q257E/PKC δ -GFP) even after 1 h of DAG-dioxolanone treatment (Figure 4C) or with higher drug concentrations (data not shown). In contrast, treatment with 1 μ M PMA induced clear plasma membrane translocation of the Q257E/PKC δ -GFP mutant immediately (within 1 min) (Figure 4D), confirming that the PKC δ remained capable of translocation in the presence of ligands that could still interact with the mutant C1b domain. Likewise, when we applied the DAG-lactone **Z-1** (20 μ M) to the C1b mutant-expressing cells, membrane translocation of the Q257E/PKC δ -GFP mutant was observed within 10 min after administration of the compound (Figure 4E). These results indicate that without ligand binding to δ C1b, δ C1a alone could not translocate the intact PKC δ to the membranes in response to DAG-dioxolanone, implying that the C1a domain does not play the major role in PKC δ redistribution. The concentration of compound **4** (20 μ M) was chosen to give a prompt, complete response to ligand addition. Typically, to achieve this goal, amounts used by researchers are appreciably higher than the measured K_i values determined *in vitro*, which represent ideal conditions for supporting the interactions. In the current studies, the objective was to show the differential pattern of response, so complete dose response curves, which are quite demanding of instrument time, were not performed.

(b) Mutating the Corresponding Glutamine Residue (Q185) in the C1a Domain of PKC δ Did Not Abolish Its Membrane Translocation in Response to DAG-dioxolanone

Treatment. To probe the role of the C1a domain, we mutated the corresponding glutamine residue in the δ C1a domain (Q185) to glutamate to generate the C1a mutant (Q185E/PKC δ -GFP). We found that, in contrast to the behavior of the C1b mutant (Q257E/PKC δ -GFP), membrane translocation of the C1a mutant (Q185E/PKC δ -GFP) was easily detected after the application of DAG-dioxolanone **4** (20 μ M) (Figure 5B), as was likewise observed for PMA (Figure 5C) and the DAG-lactone **Z-1** (Figure 5D). This result argues that the C1a domain is not necessary for translocation of PKC δ by either phorbol ester or DAG analogues in the presence of a functional C1b domain. Although the C1a/DAG-dioxolanone interaction had been inhibited in the C1a mutant, the strong C1b/DAG-dioxolanone interaction drove the whole PKC δ molecule to the membrane. However, it should be noted that without the binding to the C1a domain, the plasma membrane localization of the whole PKC δ molecule seemed to be less persistent and clear. The C1a mutant was more likely to translocate to the internal membranes. This behavior was most evident in the PMA and the DAG-lactone-treated C1a-mutant-expressing cells (Figure 5C,D). As shown in Figure 5C, the C1a mutant translocated to both the plasma membrane and the nuclear membrane in response to PMA (1 μ M), but the signal at the plasma membrane became much weaker several minutes after the translocation. In Figure 4D, we showed that with PMA the C1b mutant only translocated to the plasma membrane, where it persisted. A similar pattern could be seen for the translocation of the C1a mutant (Figure 5D) and the C1b mutant (Figure 4E) in response to the DAG-lactone. These results suggest that the C1a and C1b domains of PKC δ may play different roles in the ligand interaction and the enzyme activation by targeting the enzyme to different subcellular locations.

Discussion

As a central regulatory mechanism for a diversity of cellular functions, such as cell proliferation, differentiation, and apoptosis, the diacylglycerol signaling pathway has gained widespread attention in the biological and pharmaceutical fields.³¹ Protein kinase C (PKC), the major receptor for the DAG signal and one of the important factors in tumorigenesis,² has thus emerged as an attractive target for cancer therapy and a range of other conditions. Several strategies have been used to develop the PKC modulators. The first strategy has been inhibitors targeted to the kinase domain of the PKCs. For example, LY333531, a selective inhibitor of PKC β enzymatic activity, is currently in clinical trials for treatment of vascular complications of diabetes.^{32,33} A second strategy has been to use antisense oligonucleotides to manipulate the expression of the PKCs. For example, the PKC α antisense oligonucleotide LY900003/ISIS 3521 is currently in clinical trials.³⁴ A third strategy has been the use of compounds targeted to the C1 domains, where they are able to induce selective responses. Bryostatin 1, which is in clinical trials as a cancer chemotherapeutic agent, has a unique biphasic dose response for down-regulation and protection of PKC δ .^{35,36} 12-Deoxyphorbol 13-acetate is antitumor-promoting³⁷ and is under consideration for use in combination with HAART therapy for treatment of HIV/AIDS.³⁸ Ingenol 3-angelate, which induces biphasic induction of IL-6,³⁹ is in clinical trials for actinic keratosis and nonmelanotic skin cancer. A general rationale for this approach is that different PKC isoforms or different families of DAG receptor proteins may have antagonistic effects, depending on the system, and thus, for example, blocking PKC ϵ , an isoform that induces proliferation and is antiapoptotic, may be equivalent to stimulation of PKC δ , which is antiproliferative and proapoptotic.

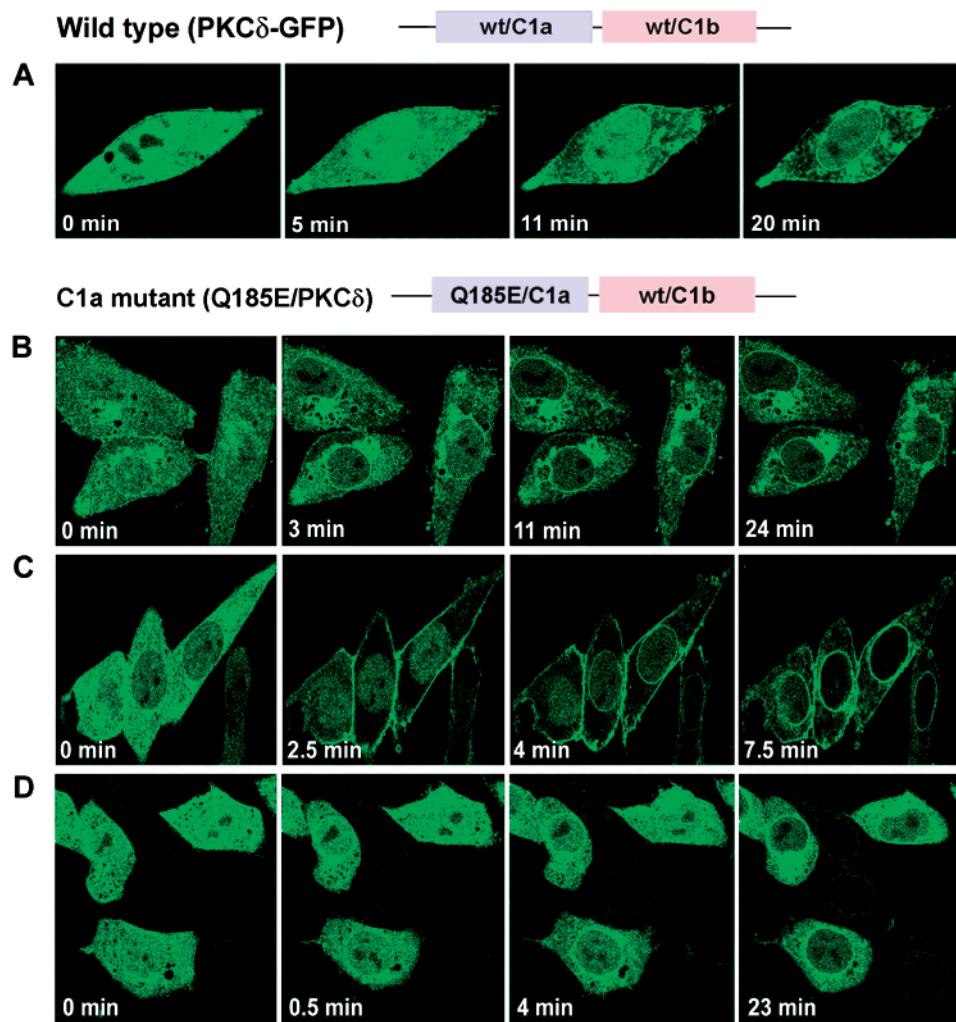


Figure 5. Confocal microscopy comparing membrane translocation of the C1a mutant (Q185E/PKC δ -GFP) of PKC δ -GFP by DAG-dioxolanone **4**, its corresponding DAG- lactone Z-1 and PMA in living CHO-K1 cells: (A) time serial images showing the dynamic translocation of wild-type PKC δ -GFP to the plasma membrane and internal membranes in living CHO-K1 cells after the application of **4** (20 μ M); (B) time serial images showing the dynamic membrane translocation of the C1a mutant (Q185E) after the application of **4** (20 μ M); (C) time serial images showing the dynamic translocation of the C1a mutant (Q185E) after the application of PMA (1 μ M); (D) time serial images showing the dynamic translocation of the C1a mutant (Q185E) after the application of corresponding DAG-lactone Z-1 (20 μ M). The minutes in each panel represent the time of drug treatment. Each experiment was performed three times with similar results.

Although natural products such as the phorbol esters, indole alkaloids, aplysiatoxin, or bryostatin have impressive potency for C1 domains, their intricate structures and multiple chiral centers have complicated their exploitation as lead structures for medicinal chemistry. Unfortunately, although the endogenous ligand for C1 domains, namely, *sn*-1,2-diacylglycerol, has a relatively simple structure with only a single chiral center, its conformational flexibility is associated with relatively weak potency. Starting with the DAG structure, our group has been able to develop DAG-lactones with in vitro potencies approaching those of the phorbol esters using a combination of conformational constraint and appropriate substitution to optimize interactions with the lipid bilayer and the rim of the C1 domain binding cleft.¹⁷ The DAG-lactones have provided a powerful template for structural modification to probe the interactions of ligands with the C1 domains. Further insights have emerged from molecular modeling, based on the X-ray structure of the complex between phorbol 13-acetate and the C1b domain of PKC δ ¹⁶ as well as from solution NMR studies.⁴⁰

As part of our effort to further enhance ligand potency and C1 domain selectivity, we have sought to identify additional potential points of interaction between DAG-lactones and the C1 domains. We described here a novel class of DAG

derivatives, DAG-dioxolanones, that were predicted from computer modeling to possess such an additional interaction site. The DAG-dioxolanones have an oxygen replacing the CH₂ in the ring structure of the DAG lactones (Table 1). The modeling predicted that this extra oxygen in the DAG-dioxolanones should be able to form an additional hydrogen bond with the glutamine residue in the C1b domain of PKC δ (Q257 in the numbering scheme for the intact PKC δ , Q27 in the numbering scheme of the isolated C1b domain as shown in Figure 1) only in the *sn*-1 binding mode involving the *sn*-1 carbonyl on the side chain. We were able to verify the importance of this predicted interaction site by mutating the indicated glutamine residue in the isolated δ C1b domain. It has been reported that the side chain of the glutamine residue is very important for the geometry of the binding cleft of the C1 domain.⁴¹ We therefore had tried to minimize the side effect of the mutation by replacing the glutamine residue (Q) with glutamate (E). Fortunately, with the glutamate residue, the binding affinity of the mutated C1b domain (Q27E/ δ C1b) for [³H]PDBu was maintained at a level with K_d in the 10⁻⁹ M range (6.2 \pm 1.0 nM), reflecting a relatively weak influence (20-fold increase in the K_d value compared with the K_d of 0.33 \pm 0.05 nM for the wild-type) of the mutation on its binding

capability for the phorbol esters. Encouragingly, our measurements on the DAG-dioxolanones demonstrated that the mutation dramatically decreased the binding affinity. For the three DAG-dioxolanones 4–6 that we had studied, the K_i values had increased from 10^{-9} M for the wild-type δ C1b to 10^{-6} M for the δ C1b mutant. However, the corresponding DAG-lactones only showed a weak decrease (35- to 55-fold of increase in the K_i values) in their binding potency for the Q27E/ δ C1b mutant (Table 2). It is thus quite clear from the above results that, as predicted by the computer modeling, the glutamine residue of the δ C1b domain does play an important role in the interaction with the DAG-dioxolanone, and this interaction is weak or nonexistent for the DAG-lactones or phorbol esters.

One objective of strategies for introducing additional points of interaction would be to further enhance potency. This objective was not met with the current DAG-dioxolanones because of their exclusive preference for the *sn*-1 binding mode that counterbalanced the entropic advantage typically observed for DAG-lactones that bind in the *sn*-2 binding mode. Simply put, the extra oxygen in DAG-dioxolanones forms an effective hydrogen bond with glutamine (Q27E) only when it binds in the *sn*-1 mode. Therefore, despite this additional hydrogen bond (Figure 1), the binding affinities of these new DAG derivatives were not increased relative to the corresponding DAG-lactones, neither for the intact PKC α (Table 1) nor for the isolated C1b domain of PKC δ (Table 2). Rather, there was a several-fold decrease in their binding affinities (Tables 1 and 2). Since the mutation of the glutamine residue (Q27E/ δ C1b) much more strongly reduced the binding potencies of the DAG-dioxolanone than of the DAG lactones, a plausible explanation is that the δ C1b domain is able to retain binding to the DAG-lactones even after mutation, whereas interactions between the mutated Glu27 residue and the DAG-dioxolanone are so unfavorable that binding is lost.

The DAG-responsive PKC and PKD isoforms possess twin C1 domains. Their relative contributions to PKC function, despite considerable analysis, still remain unresolved, with different methodological approaches yielding different conclusions. For example, in terms of binding affinity, initial studies showed that both C1 domains of PKC γ bound PDBu with high affinity, indicating that the C1a and C1b of PKC γ are functionally equivalent.^{7,42} By expressing the truncated PKC α in the yeast *Saccharomyces cerevisiae*, Riedel's group found that the presence of either C1 domain allowed phospholipid and phorbol ester regulation of PKC α enzymatic activity, implying an equal function of the C1a and C1b domains in PKC α .⁴³ In contrast, later investigations suggested that the two C1 domains function differently in PKC activation. Cho and co-workers described that the hydrophobic residues in the C1a domain were essential for the membrane penetration and activation of PKC α , whereas those in the C1b domain were not directly involved in these processes.⁴⁴ Using dimeric bisphorbols, Newton's group demonstrated that both C1 domains of PKC β were oriented for potential membrane interaction but only one C1 domain bound ligand in a physiological context.⁴⁵ With synthetic C1 peptides, Irie's group reported different binding affinities of the C1a and C1b domains of different PKC isoforms for various ligands.^{46,47} Our previous work has demonstrated differential roles of the C1a and C1b domains in translocation and down-regulation of PKC δ , with different responses for different ligands.^{48,49}

The combination of the DAG-dioxolanones and the Q257E mutation provides a powerful tool for addressing the role of ligand binding to the C1 domain in PKC functioning. An underlying problem with deletion of an entire C1 domain or of

mutations that abrogate binding activity (e.g., P11G, numbered according to the sequence of the isolated C1 domain) is the lack of a positive control to distinguish the effect of the alteration itself from the lack of recognition of ligand. Because the Q27E mutation selectively blocks response to the DAG-dioxolanone but not phorbol ester or DAG-lactone, comparison of the response of the mutated PKC δ to these ligands provides a test for the function of the C1b domain. We showed (Figures 4 and 5) that when we abolished the C1b/dioxolanone interaction by mutating the indicated glutamine residue (Q257) in the C1b domain, the whole PKC δ enzyme no longer translocated to the membranes in response to DAG-dioxolanone 4 (Figure 4C). Since DAG-dioxolanone 4 bound with good affinity to the wild-type C1a domain of PKC δ (K_i value of 4.31 ± 0.13 nM, Table 3), the lack of translocation of the C1b mutant (Q257E/PKC δ) by the DAG-dioxolanone indicates that the C1a-dioxolanone interaction by itself was unable to drive translocation of the whole PKC δ protein to the membranes, at least over the ligand range examined. The C1b/dioxolanone interaction would thus appear to be the major force for driving the membrane translocation of the whole PKC δ enzyme. This conclusion was consistent with our results with the C1a mutant of PKC δ (Q185E/PKC δ). Although this aspect of the analysis is less robust, in that the mutation markedly reduces the potency of the C1a domain for the other ligands as well, depriving us of a positive control (Table 3), the retention of translocation of the mutated PKC δ enzyme again argues that the C1a/ligand interaction is not critical for the membrane translocation of the whole PKC δ enzyme in response to these ligands.

Close examination of the data is consistent, in any case, with a secondary contribution of the C1a domain of PKC δ to the membrane site to which PKC δ translocates. In response to 1 μ M PMA, the C1a mutant (Q185E) (functional C1b domain, reduced affinity at the C1a domain for PMA) translocated to both plasma membrane and the nuclear membrane (Figure 5C), whereas the C1b mutant (Q257E) (functional C1a domain, reduced affinity at the C1b domain for PMA) only translocated to the plasma membrane in response to PMA (Figure 4D). No nuclear membrane translocation could be seen even after 1 h of the PMA treatment (data not shown). For the native PKC δ , DAG-lactones cause translocation to both plasma membrane and the nuclear membrane (data not shown). In response to the DAG-lactone, the C1b mutant only translocated to the plasma membrane (Figure 4 E), whereas the C1a mutant only translocated to the nuclear membrane (Figure 5 D). The results presumably reflect the reduced affinity of the mutated C1 domain for the phorbol ester or DAG-lactone, with the C1a domain favoring plasma membrane localization and the C1b domain being less selective. They also emphasize that both domains influence translocation of PKC δ , even if the C1b domain plays the predominant role.

It has been suggested elsewhere that phorbol esters and DAG interact with different C1 domains, with the phorbol ester interacting with the C1b domain and the DAG interacting with the C1a domain.⁵⁰ Our results argue that this is not of major importance for translocation of PKC δ and that the C1b domain plays the predominant role for the DAG-lactones as well as for the phorbol esters.

The high conservation of phorbol ester binding affinity across species as diverse as nematodes, drosophila, and man had suggested that different C1 domains should show very similar characteristics for ligand recognition. Emerging evidence from multiple groups, however, emphasizes impressive diversity among the properties of different C1 domains.^{45,46,48} For

example, we described that the RasGRP-selective DAG-lactone 130C037 bound with high affinity to the C1b domain of PKC δ but with orders of magnitude lower affinity to the C1a domain of PKC δ or to either C1 domain of PKC α .¹⁹ The substantially different effect of the mutation Q27E for the C1a domain of PKC δ , where it had no differential effect on binding of the DAG-dioxolanone compared to the DAG-lactone or the phorbol ester, provides yet another example of this diversity.

In a summary, our results described here again illustrate the power of the DAG-lactone template as a platform for exploration of ligand–C1 domain interactions. Understanding of these interactions is central to the rational design of ligands selective for PKC isoforms or other members of the families of proteins with C1 domains that mediate signaling downstream of the lipophilic second messenger DAG. These proteins represent promising therapeutic targets, given both their biological functions and the actions of agents currently under development.

Experimental Section

Materials and General Procedures. All reagents for chemical syntheses were commercially available. [20-³H]Phorbol 12,13-dibutyrate ([³H]PDBu) (20 Ci/mmol) was purchased from Perkin-Elmer (Boston, MA). PDBu and phorbol 12-myristate-13-acetate (PMA) were purchased from LC Laboratories (Woburn, MA). Phosphatidyl-L-serine was purchased from Avanti Polar Lipids (Alabaster, AL). Reagents for expression and purification of glutathione *S*-transferase (GST) fusion proteins were obtained from Pierce Biotechnology, Inc. (Rockford, IL). Cell culture medium and reagents and the DNA primers were obtained from Invitrogen (Carlsbad, CA). Recombinant mouse PKC α was expressed and partially purified as described elsewhere.⁵¹ Melting points were determined on a MelTemp II apparatus, Laboratory Devices, and are uncorrected. Column chromatography was performed on silica gel 60, 230–400 mesh (E. Merck or Bodman Industries), and analytical TLC was performed on Analtech Uniplates silica gel GF. ¹H and ¹³C NMR spectra were recorded on a Varian Unity Inova instrument at 400 and 100 MHz, respectively. Spectra are referenced to the solvent in which they were run (7.26 ppm for CDCl₃). Positive-ion fast atom bombardment mass spectra (FABMS) were obtained on a VG 7070E-HF double-focusing mass spectrometer operated at an accelerating voltage of 6 kV under the control of a MASPEC-II data system for Windows (Mass Spectrometry Services, Ltd.). Either glycerol or 3-nitrobenzyl alcohol was used as the sample matrix, and ionization was effected by a beam of xenon atoms generated in a saddle-field ion gun at 8.0 ± 0.5 kV. Nominal mass spectra were obtained at a resolution of 1200, and matrix-derived ions were background-subtracted during data system processing. Elemental analyses were performed by Atlantic Micro-lab, Inc., Norcross, GA. The partition coefficients (log *P*) were calculated according to the atom-based program MOE SLog P.²³

Construction and Purification of GST-Fused C1 Domains of PKC α and PKC δ in *E. coli*. The C1a and C1b domains of PKC δ were generated by polymerase chain reaction (PCR) using the Platinum *Pfx* DNA polymerase (Invitrogen). The full-length cDNA clone of murine PKC δ was used as the template. The following oligonucleotides were used as the PCR primers to pull out the targeted C1 domains: (1) forward and reverse primers for δ C1a were 5'-AAACAGGCCAAGATCCACTACA-3' and 5'-GGTGTCCCGCTATTGGT-3'; (2) forward and reverse primers for δ C1b were 5'-CAGAAAGAACGCTTCAACATCG-3' and 5'-GGCCTCAGCCAAGAGCTTT-3'. The blunt-ended PCR products were ligated into a pCR-Blunt vector using the Zero Blunt PCR cloning kit (Invitrogen). The pCR-Blunt vector was digested with EcoRI (New England BioLabs, Inc., Beverly, MA) to produce adhesive ends of the C1 fragment. This fragment was then ligated into the appropriate glutathione *S*-transferase (GST)-containing vectors (i.e., pGEX-5X-1, pGEX-5X-2, pGEX-5X-3) (Amersham Biosciences, Piscataway, NJ), using the EcoRI restriction sites with the sequence of the insert in the intended reading frame. The DNA sequence of

each construct was finally confirmed by sequence analysis (DNA Minicore, Center for Cancer Research, NCI, NIH).

After construction, the recombinant plasmids of individual C1 domains of PKC δ were transformed into BL-21-Gold (DE3) *E. coli* competent cells (Stratagene, La Jolla, CA). The expression of the GST-fusion proteins was induced by the addition of 0.5 mM isopropyl-*O*-D-thiogalactopyranoside (IPTG) when the OD of the LB medium reached 0.5–0.7. The bacteria were harvested after 4 h of induction at 37 °C. The expressed GST-tagged C1 protein was purified using a B-PER GST spin purification kit according to the manufacturer's instructions (Pierce Biotechnology, Inc., Rockford, IL). The purity of the protein was verified by SDS-PAGE and staining with Coomassie Blue. The protein concentration was measured using the Bio-Rad protein assay kit according to the manufacturer's instructions (Bio-Rad, Hercules, CA). The purified GST-C1 protein was stored in 30% glycerol at –70 °C.

Site-Directed Mutagenesis of the C1 Domains of PKC δ . Mutagenesis of the glutamine residue in the C1a and C1b domains of PKC δ was performed in the isolated GST- δ C1a, GST- δ C1b, and the intact PKC δ -GFP proteins using the QuikChange II site-directed mutagenesis kit (Stratagene) according to the manufacturer's instructions. The C1 domain containing pGEX plasmid or the intact PKC δ containing pEGFP plasmid was used as the template for the mutagenesis reactions. The glutamine/glutamate mutagenic primers for the δ C1b domain were 5'-GGGACTGGTGAAGGAGGGATTAAAGTGTGAAG-3' (sense) and 5'-CTTCACTTTAATCCCTCCTTACCAGTCCC-3' (antisense). The mutagenic primers for the δ C1a domain were 5'-GGCCTCAAACAAGGAAGGCTACAAATGCAGG-3' (sense) and 5'-CCTGCATTGTAGCCTTCCTTGTGAGGCC-3' (antisense). The mutated codons are underlined. The mutation was confirmed by DNA sequence analysis (DNA Minicore, Center for Cancer Research, NCI, NIH). The mutated plasmids were used to express the corresponding GST or GFP fusion proteins, which were purified or used in the experiments as described elsewhere in this study.

[³H]PDBu Binding Assay. Enzyme–ligand interactions were assessed in terms of the ability of the ligand to displace bound [20-³H]phorbol 12,13-dibutyrate (PDBu) from a recombinant single isozyme (PKC α) in the presence of phosphatidylserine.^{52–56} [³H]-PDBu binding to the recombinant full-length PKC α or the individual C1 domains was measured using the polyethylene glycol precipitation assay developed in our laboratory as described elsewhere.⁵² Briefly, the assay mixture (250 μ L) contained 50 mM Tris-HCl (pH 7.4), 100 μ g/mL phosphatidylserine, 4 mg/mL bovine immunoglobulin G, [³H]PDBu, and various concentrations of competing ligand. Incubation was carried out at 37 °C for 5 min (for full-length PKC isoforms) or 18 °C for 10 min (for C1 domains). Samples were chilled on ice for 7 min, and 200 μ L of 35% polyethylene glycol in 50 mM Tris-HCl (pH 7.4) was added. The samples were mixed and incubated on ice for an additional 10 min. The tubes were centrifuged in a Beckman Allegra 21R centrifuge at 4 °C (12 200 rpm, 15 min). A 100 μ L aliquot of the supernatant was removed for the determination of the free concentration of [³H]PDBu, and the pellet was carefully dried. The tip of the centrifuge tube containing the pellet was cut off and transferred to a scintillation vial for the determination of the total bound [³H]PDBu. Cytoscint (ICN, Costa Mesa, CA) was added to both an aliquot of the supernatant and the pellet. Radioactivity was determined by scintillation counting. Specific binding was calculated as the difference between total and nonspecific binding. Standard Scatchard analysis was performed to determine the dissociation constants (*K*_d) of the individual C1 domains, and the inhibitory dissociation constants (*K*_i) were calculated using our standard method as described previously.⁵²

Expression and Imaging of the GFP-Tagged PKC Proteins in Live CHO Cells. CHO-K1 cells (obtained from ATCC, Manassas, VA) were cultured at 37 °C in F-12 (HAM) nutrient containing 10% FBS, penicillin (50 units/mL), and streptomycin (0.05 mg/mL) in a 5% CO₂ atmosphere. The plasmid DNA of GFP-fused PKC proteins was transfected into the CHO-K1 cells using Lipofectamine 2000 (Invitrogen) according to the manufacturer's

instructions. The expression of the fluorescent protein was detected 24 h after transfection. Confocal fluorescent images were collected with a Bio-Rad MRC 1024 confocal scan head (Bio-Rad) mounted on a Nikon microscope with a 60 \times planapochromat lens. Excitation at 488 nm was generated by a krypton–argon gas laser with a 522/32 emission filter for green fluorescence. For kinetics of PKC-GFP translocation in live cells, cells plated on a 40 mm round coverslip were enclosed in a Biopetechs Focht Chamber System (Biopetechs, Butler, PA). The chamber was inverted and attached to the microscope stage with a custom stage adapter. A temperature controller set at 37 °C was connected, and medium was perfused through the chamber with a Lambda microperfusion pump. Sequential images of the same cell were collected at various time points using LaserSharp Software (Bio-Rad).

Docking of DAG-dioxolanones into the C1b Domain of PKC δ . Structures for all compounds were built in SYBYL⁵⁷ and minimized with the MMFF94 force field and partial charges.⁵⁸ Docking was then performed using FlexX⁵⁹ through its SYBYL module into the crystal structure of the C1b domain of PKC δ .¹⁶ The binding site was defined as residues 238–243, 250–254, and 257. The ring structure in the ligand was treated flexibly, and all other options were set to their default values.

Homology Modeling of the C1a Domain of PKC δ and the Q27E Mutants. A homology model of the C1a domain of PKC δ was built on the backbone coordinates of the crystal structure of the C1b domain.¹⁶ Side chains for the model were constructed using the program SCWRL,⁶⁰ which uses a backbone-dependent rotamer library to place residues in their most likely conformation given the backbone ϕ – ψ angles at that position. Residues homologous to PKC δ were left unchanged from their crystallographic positions. The model was refined with a small energy minimization, with phorbol 13-*O*-acetate left in position from the crystal structure to prevent the binding site loops from closing during the minimization. Harmonic positional restraints on the backbone atoms were gradually relaxed over the course of the minimization to eliminate steric clashes in the side chains without inducing deformations in the backbone.

Structures for the mutant Q27E C1a and C1b domains were built by simply replacing the glutamine residue at position 27 in the structure with a glutamate residue, without any subsequent minimization or other refinement.

Molecular Dynamics with an Implicit Solvent Bilayer. Simulations were run in CHARMM,⁶¹ version c32b2, using the all-hydrogen force field parameter set for proteins⁶² with backbone dihedral corrections.⁶³ Additional parameters for the DAG-lactones and DAG-dioxolanones were developed by analogy with existing parameters for lipids and furanose sugars and were checked against ab initio geometry-optimized structures calculated at the RHF/6-31G* theory level.

The implicit solvent was modeled using the GBSW module (generalized Born with a simple switching function²⁹). A low-dielectric, solvent-inaccessible planar slab perpendicular to the *z*-axis was set up at *z* = 0. The thickness of the slab was 25.0 Å, and the width of the smoothing region between the membrane and water environments was 5.0 Å. In this smoothing region, a polynomial function is used to scale the solvent (water) accessibility from 0 inside the membrane to 1 outside, which gives an approximation of the dielectric characteristics of a real membrane bilayer. For the polar portion of the solvation energy, the external solvent dielectric constant was set to 80.0 and the internal dielectric constant of the protein was set to 1.0, with a smoothing length of 0.6 Å at the boundary between the two. Optimized atomic Born radii⁶⁴ were used to define the dielectric boundary at the protein surface. The surface tension coefficient for the nonpolar portion of the solvation energy was 0.04 kcal mol⁻¹ Å⁻².

We began with structures for DAG-lactone **Z-1** and DAG-dioxolanone **Z-4**, in both the *sn*-1 and *sn*-2 binding modes, docked into the PKC δ C1b domain, the homology model of the PKC δ C1a domain, and models of the mutant Q27E C1b and C1a domains, for a total of 16 systems. Weak constraints were included to hold the distance between the atoms involved in the three conserved hydrogen bonds between the ligands and the protein at less than

3.0 Å in order to keep the ligand in the binding site and to preserve its *sn*-1 or *sn*-2 orientation. Without these restraints, ligands tended to drift in and out of the binding site and switch binding orientations (data not shown).

Each system first underwent 25 steps of steepest descent minimization with the ligand atoms and protein backbone atoms fixed in place, followed by 100 steps of adopted-basis Newton–Raphson minimization with harmonic constraints on the backbone atoms and finally 200 steps of adopted-basis Newton–Raphson minimization with no constraints. The systems were then heated in 10 K increments every 0.2 ps from a starting temperature of 50 to 300 K and equilibrated at 300 K for 100 ps. After equilibration, data were collected over the course of 10 ns, with coordinates written to disk at 100 ps intervals to give an ensemble of 100 structure snapshots for each system.

The hydrogen-bonding energy for each system was calculated in CHARMM by first defining four subsets consisting of ligand donor atoms, ligand acceptor atoms, receptor donor atoms, and receptor acceptor atoms. Each potential donor–acceptor pair was tested to see whether it was within allowable hydrogen-bonding geometry, i.e., with an H \cdots A distance of 2.7 Å or less and a D–H \cdots A angle greater than 90°. If so, the nonbonded (electrostatic and van der Waals) interaction energy between the two atoms was calculated. The sum of these interaction energies for all the snapshots in the ensemble was then divided by 100 to give the average hydrogen-bonding energy for the ensemble.

E- and Z-5-[(4-Methoxyphenoxy)methyl]-3-(3-methylbutylidene)-5-[(phenylmethoxy)methyl]-4,5-dihydrofuran-2-one (VI, R = CH₂CH(CH₃)₂). Lithium bis(trimethylsilyl)amide (LHMDS, 5.4 mL, 5.4 mmol, 1 M in THF) was added dropwise to a –78 °C stirring solution of **IV**^{20,21} (920 mg, 2.7 mmol) in THF (10 mL). After 10 min, the mixture was treated with isovaleryl aldehyde (0.29 mL, 2.7 mmol) and stirred at the same temperature for 20 min. The reaction mixture was then quenched by slow addition of saturated aqueous NH₄Cl and extracted with Et₂O (3 \times). The combined organic layers were then washed with water (1 \times) and brine (1 \times), dried over MgSO₄, and concentrated in vacuo. The residue was purified by flash column chromatography on silica gel with EtOAc/hexanes (1:4) to give **V** (R = CH₂CH(CH₃)₂), which was used immediately without further purification or characterization. This compound was taken up in CH₂Cl₂ (20 mL) and treated with Et₃N (1.1 mL, 8.1 mmol) and methanesulfonyl chloride (0.31 mL, 4.1 mmol). After the mixture was stirred for 10 min at room temperature, DBU (1.2 mL, 8.1 mmol) was added and the mixture was stirred overnight. Concentration followed by purification by silica gel chromatography with EtOAc/hexanes (1:6) gave **Z-VI** (R = CH₂CH(CH₃)₂, 260 mg, 23%) and **E-VI** (R = CH₂CH(CH₃)₂, 512 mg, 46%) as a mixture of isomers that were separated via column chromatography.

Z-VI (R = CH₂CH(CH₃)₂). ¹H NMR (CDCl₃) δ 7.27–7.36 (m, 5 H, PhCH₂OCH₂), 6.83 (s, 4 H, MeOC₄H₄OCH₂), 6.24 (tt, 1 H, *J* = 7.8, 2.3 Hz, C=CHCH₂CH(CH₃)₂), 4.60 (AB q, 2 H, *J* = 12.1 Hz, PhCH₂OCH₂), 4.03 (AB q, *J* = 9.8 Hz, 2 H, MeOC₄H₄OCH₂), 3.76 (s, 3 H, MeOC₄H₄OCH₂), 3.68 (AB q, *J* = 10.2 Hz, 2 H, PhCH₂OCH₂), 2.91 (AB qm, *J* = 16.5, 2 H, H-4_{ab}), 2.64–2.68 (m, 2 H, C=CHCH₂CH(CH₃)₂), 1.75 (sept, 1 H, *J* = 6.7 Hz, C=CHCH₂CH(CH₃)₂), 0.96 and 0.97 (d, *J* = 6.7 Hz, 6 H, C=CHCH₂CH(CH₃)₂). FAB-MS (*m/z*, relative intensity): 411 (MH⁺, 45), 410 (M⁺, 74), 91 (100), Anal. (C₂₅H₃₀O₅) C, H.

E-VI (R = CH₂CH(CH₃)₂). ¹H NMR (CDCl₃) δ 7.24–7.34 (m, 5 H, PhCH₂OCH₂), 6.80 (s, 4 H, MeOC₄H₄OCH₂), 6.77 (tt, 1 H, *J* = 7.7, 2.8 Hz, C=CHCH₂CH(CH₃)₂), 4.57 (AB q, 2 H, *J* = 12.1 Hz, PhCH₂OCH₂), 4.03 (AB q, *J* = 9.8 Hz, 2 H, MeOC₄H₄OCH₂), 3.74 (s, 3 H, MeOC₄H₄OCH₂), 3.67 (AB q, *J* = 10.2 Hz, 2 H, PhCH₂OCH₂), 2.91 (AB qm, *J* = 17.1, 2 H, H-4_{ab}), 2.01–2.08 (m, 2 H, C=CHCH₂CH(CH₃)₂), 1.80 (sept, *J* = 6.7 Hz, 1 H, C=CHCH₂CH(CH₃)₂), 0.933 and 0.930 (d, *J* = 6.7 Hz, 6 H, C=CHCH₂CH(CH₃)₂). FAB-MS (*m/z*, relative intensity): 411 (MH⁺, 45), 410 (M⁺, 74), 91 (100), Anal. (C₂₅H₃₀O₅) C, H.

Z- and E-5-[(4-Methoxyphenoxy)methyl]-3-[5-methyl-3-(2-methylpropyl)hexylidene]-5-[(phenylmethoxy)methyl]-4,5-dihy-

drofuran-2-one (VI, R = CH₂CH(CH₂CH(CH₃)₂)₂. These compounds have been previously reported.²¹

General Procedure for Removing the PMP Group. Ceric ammonium nitrate (CAN, 3 equiv) was added to a 0 °C stirring solution of VI (1 equiv) in CH₃CN/H₂O (4:1, 9 mL/mmol). After 15 min, the reaction was quenched with aqueous saturated NaHCO₃, extracted with EtOAc, dried over MgSO₄, and concentrated in vacuo. Purification by silica gel chromatography with hexanes/EtOAc (2:1) gave VII, which was carried through to the next step without further characterization.

Z-5-(Hydroxymethyl)-3-(3-methylbutylidene)-5-[(phenylmethoxy)methyl]-4,5-dihydrofuran-2-one (Z-VI, R = CH₂CH(CH₃)₂). According to the general procedure, Z-VI (R = CH₂CH(CH₃)₂, 260 mg, 0.63 mol) was combined with CAN (1.0 mg, 1.89 mmol) to give Z-VII (R = CH₂CH(CH₃)₂, 196 mg, 100%) as a colorless oil. ¹H NMR (CDCl₃) δ 7.27–7.36 (m, 5 H, PhCH₂OCH₂), 6.20 (tt, *J* = 7.8, 2.3 Hz, 1 H, C=CHCH₂CH(CH₃)₂), 4.55 (AB q, 2 H, *J* = 11.9 Hz, PhCH₂OCH₂), 3.66 and 3.74 (dd, *J* = 12.1, 6.4 Hz, 2 H, HOCH₂), 3.56 (AB q, 2 H, *J* = 10.1 Hz, PhCH₂OCH₂), 2.82 (app q, 2 H, C=CHCH₂CH(CH₃)₂), 2.53–2.67 (m, 2 H, H-4_{ab}), 2.41 (t, *J* = 6.6 Hz, 2 H, HOCH₂), 1.81 (sept, *J* = 6.7 Hz, 1 H, C=CHCH₂CH(CH₃)₂), 0.92 and 0.91 (d, *J* = 6.7 Hz, 6 H, C=CHCH₂CH(CH₃)₂).

E-5-(Hydroxymethyl)-3-(3-methylbutylidene)-5-[(phenylmethoxy)methyl]-4,5-dihydrofuran-2-one (E-VI, R = CH₂CH(CH₃)₂). According to the general procedure, E-VI (R = CH₂CH(CH₃)₂, 512 mg, 0.12 mol) was combined with CAN (1.9 mg, 3.6 mmol) to give E-VII (R = CH₂CH(CH₃)₂, 392 mg, 100%) as a white solid: mp 44–45 °C; ¹H NMR (CDCl₃) δ 7.24–7.34 (m, 5 H, PhCH₂OCH₂), 6.72 (tt, *J* = 7.7, 2.9 Hz, 1 H, C=CHCH₂CH(CH₃)₂), 4.54 (s, 2 H, PhCH₂OCH₂), 3.74 (dd, *J* = 12.1, 6.5 Hz, 1 H, HOCHH), 3.64 (dd, *J* = 12.1, 6.4 Hz, 2 H, HOCHH), 3.56 (AB q, *J* = 10.1 Hz, 2 H, PhCH₂OCH₂), 2.80 (t, *J* = 6.5, 1 H, HOCH₂), 2.73 (m, 2 H, C=CHCH₂CH(CH₃)₂), 2.02–2.06 (m, 2 H, H-4_{ab}), 1.78 (sept, *J* = 6.7 Hz, 1 H, C=CHCH₂CH(CH₃)₂), 0.92 and 0.91 (d, *J* = 6.7 Hz, 6 H, C=CHCH₂CH(CH₃)₂).

Z-5-(Hydroxymethyl)-3-[5-methyl-3-(2-methylpropyl)hexylidene]-5-[(phenylmethoxy)methyl]-4,5-dihydrofuran-2-one (Z-VII, R = CH₂CH(CH₂CH(CH₃)₂)₂). According to the general procedure, Z-VI (R = CH₂CH(CH₂CH(CH₃)₂)₂, 379 mg, 0.77 mol) was combined with CAN (1.26 g, 2.3 mmol) to give Z-VII (R = CH₂CH(CH₂CH(CH₃)₂)₂, 298 mg, 98%). This compound has been previously reported.²¹

E-5-(Hydroxymethyl)-3-[5-methyl-3-(2-methylpropyl)hexylidene]-5-[(phenylmethoxy)methyl]-4,5-dihydrofuran-2-one (E-VII, R = CH₂CH(CH₂CH(CH₃)₂)₂). According to the general procedure, E-VI (R = CH₂CH(CH₂CH(CH₃)₂)₂, 135 mg, 0.27 mol) was combined with CAN (448 mg, 0.81 mmol) to give E-VII (R = CH₂CH(CH₂CH(CH₃)₂)₂, 87 mg, 81%). This compound has been previously reported.²¹

General Procedure for Acylation. A solution of VII (1 equiv) in CH₂Cl₂ (5 mL/mmol) was treated with Et₃N (3 equiv), acid chloride (1.5 equiv), and catalytic DMAP. After being stirred for 10 min, the mixture was concentrated in vacuo and the residue was purified by silica gel chromatography with EtOAc/hexanes (1:7) to give VIII.

Z-{4-(3-Methylbutylidene)-5-oxo-2-[(phenylmethoxy)methyl]-2-(2,3-dihydrofuryl)}methyl 5-Methyl-3-(2-methylpropyl)hexanoate (Z-VIII, R = CH₂CH(CH₃)₂, R' = CH₂CH(CH₂CH(CH₃)₂)₂). According to the general procedure, Z-VII (R = CH₂CH(CH₃)₂, 196 mg, 0.63 mmol) was combined with 5-methyl-3-(2-methylpropyl)hexanoyl chloride (128 mg, 0.63 mmol) to give Z-VIII (R = CH₂CH(CH₃)₂, R' = CH₂CH(CH₂CH(CH₃)₂)₂, 127 mg, 43%) as a colorless oil, which was contaminated with a small amount of the *E*-isomer that was formed under the reaction conditions. FAB-MS (*m/z*, relative intensity): 473 (MH⁺, 38), 91 (100). Anal. (C₂₉H₄₄O₅·0.5H₂O) C, H.

E-{4-(3-Methylbutylidene)-5-oxo-2-[(phenylmethoxy)methyl]-2-(2,3-dihydrofuryl)}methyl 5-Methyl-3-(2-methylpropyl)hexanoate (E-VIII, R = CH₂CH(CH₃)₂, R' = CH₂CH(CH₂CH(CH₃)₂)₂). According to the general procedure, E-VII (R =

CH₂CH(CH₃)₂, 392 mg, 1.2 mmol) was combined with 5-methyl-3-(2-methylpropyl)hexanoyl chloride (245 mg, 1.2 mmol) to give E-VIII (R = CH₂CH(CH₃)₂, R' = CH₂CH(CH₂CH(CH₃)₂)₂, 265 mg, 47%) as a colorless oil. ¹H NMR (CDCl₃) δ 7.26–7.35 (m, 5 H, PhCH₂OCH₂), 6.75 (tt, *J* = 7.7, 2.8 Hz, 1 H, C=CHCH₂CH(CH₃)₂), 4.55 (s, 2 H, PhCH₂OCH₂), 4.21 (s, 2 H, (CH₃)₂CHCH₂CHCH₂CO₂CH₂), 3.55 (AB q, *J* = 10.0 Hz, 2 H, PhCH₂OCH₂), 2.73 (AB qm, 2 H, *J* = 17.1 Hz, H-3_{ab}), 2.18–2.20 (m, 2 H, (CH₃)₂CHCH₂CHCH₂CO₂CH₂), 2.04 (app t, 1 H, C=CHCH₂CH(CH₃)₂), 1.91 (app p, 2 H, (CH₃)₂CHCH₂CHCH₂CO₂CH₂), 1.79 (app sept, 1 H, C=CHCH₂CH(CH₃)₂), 1.51–1.64 (m, 2 H, (CH₃)₂CHCH₂CHCH₂CO₂CH₂), 1.02–1.14 (m, 4 H, (CH₃)₂CHCH₂CHCH₂CO₂CH₂), 0.93 and 0.92 (d, *J* = 6.6 Hz, 6 H, C=CHCH₂CH(CH₃)₂), 0.84–0.87 (m, 12 H, (CH₃)₂CHCH₂CHCH₂CO₂CH₂). FAB-MS (*m/z*, relative intensity): 473 (MH⁺, 24), 91 (100). Anal. (C₂₉H₄₄O₅·0.5H₂O) C, H.

Z-{4-[5-Methyl-3-(2-methylpropyl)hexylidene]-5-oxo-2-[(phenylmethoxy)methyl]-2-(2,3-dihydrofuryl)}methyl 3-Methylbutanoate (Z-VIII, R = CH₂CH(CH₂CH(CH₃)₂)₂, R' = CH₂CH(CH₃)₂). According to the general procedure, Z-VII (R = CH₂CH(CH₂CH(CH₃)₂)₂, 298 mg, 0.76 mmol) was combined with isovaleryl chloride (0.14 mL, 1.1 mmol) to give Z-VIII (R = CH₂CH(CH₂CH(CH₃)₂)₂, R' = CH₂CH(CH₃)₂, 309 mg, 86%) as a colorless oil. ¹H NMR (CDCl₃) δ 7.27–7.36 (m, 5 H, PhCH₂OCH₂), 6.20 (tt, 1 H, *J* = 7.5, 2.2 Hz, C=CHCH₂CH(CH₂CH(CH₃)₂)₂), 4.56 (s, 2 H, PhCH₂OCH₂), 4.22 (AB q, 2 H, *J* = 11.9 Hz, (CH₃)₂CHCH₂CO₂CH₂), 3.54 (AB q, 2 H, *J* = 9.9 Hz, PhCH₂OCH₂), 2.82 (AB qm, 2 H, *J* = 16.4 Hz, H-3_{ab}), 2.65–2.69 (m, 2 H, C=CHCH₂CH(CH₂CH(CH₃)₂)₂), 2.17–2.19 (m, 2 H, (CH₃)₂CHCH₂CO₂CH₂), 2.00–2.12 (m, 1 H, (CH₃)₂CHCH₂CO₂CH₂), 1.57–1.70 (m, 3 H, C=CHCH₂CH(CH₂CH(CH₃)₂)₂), 0.99–1.11 (m, 4 H, C=CHCH₂CH(CH₂CH(CH₃)₂)₂), 0.94 and 0.93 (s, 6 H, (CH₃)₂CHCH₂CO₂CH₂), 0.84–0.87 (m, 12 H, C=CHCH₂CH(CH₂CH(CH₃)₂)₂). FAB-MS (*m/z*, relative intensity): 473 (MH⁺, 27), 91 (100). Anal. (C₂₉H₄₄O₅) C, H.

E-{4-[5-Methyl-3-(2-methylpropyl)hexylidene]-5-oxo-2-[(phenylmethoxy)methyl]-2-(2,3-dihydrofuryl)}methyl 3-Methylbutanoate (E-VIII, R = CH₂CH(CH₂CH(CH₃)₂)₂, R' = CH₂CH(CH₃)₂). According to the general procedure, E-VII (R = CH₂CH(CH₂CH(CH₃)₂)₂, 87 mg, 0.22 mmol) was combined with isovaleryl chloride (0.04 mL, 0.33 mmol) to give E-VIII (R = CH₂CH(CH₂CH(CH₃)₂)₂, R' = CH₂CH(CH₃)₂, 103 mg, 100%) as a colorless oil. ¹H NMR (CDCl₃) δ 7.27–7.36 (m, 5 H, PhCH₂OCH₂), 6.77 (tt, *J* = 7.6, 2.8 Hz, 1 H, C=CHCH₂CH(CH₂CH(CH₃)₂)₂), 4.55 (s, 2 H, PhCH₂OCH₂), 4.23 (AB q, *J* = 11.9 Hz, 2 H, (CH₃)₂CHCH₂CO₂CH₂), 3.55 (AB q, *J* = 9.9 Hz, 2 H, PhCH₂OCH₂), 2.73 (AB qm, 2 H, *J* = 17.1 Hz, H-3_{ab}), 2.16–2.18 (m, 2 H, (CH₃)₂CHCH₂CO₂CH₂), 2.01–2.16 (m, 3 H, C=CHCH₂CH(CH₂CH(CH₃)₂)₂ and (CH₃)₂CHCH₂CO₂CH₂), 1.57–1.73 (m, 3 H, C=CHCH₂CH(CH₂CH(CH₃)₂)₂), 1.06–1.12 (m, 4 H, C=CHCH₂CH(CH₂CH(CH₃)₂)₂), 0.94 and 0.92 (s, 6 H, (CH₃)₂CHCH₂CO₂CH₂), 0.87 and 0.85 (m, 12 H, C=CHCH₂CH(CH₂CH(CH₃)₂)₂). FAB-MS (*m/z*, relative intensity): 473 (MH⁺, 25), 91 (100). Anal. (C₂₉H₄₄O₅) C, H.

General Procedure for Removal of the Benzyl Ether Group. A solution of BCl₃ (3 equiv, 1 M in CH₂Cl₂) was added to a –78 °C stirring solution of VIII (1 equiv) in CH₂Cl₂ (10 mL/mmol), and the reaction was monitored by TLC. Upon completion, the reaction mixture was quenched with saturated aqueous NaHCO₃, warmed to room temperature, and extracted with CH₂Cl₂ (2×). Concentration in vacuo followed by purification by silica gel chromatography with EtOAc/hexanes gave IX.

Z-{2-(Hydroxymethyl)-4-[5-methyl-3-(2-methylpropyl)hexylidene]-5-oxo-2-(2,3-dihydrofuryl)}methyl 3-Methylbutanoate (Z-2). According to the general procedure, Z-VIII (R = CH₂CH(CH₂CH(CH₃)₂)₂, R' = CH₂CH(CH₃)₂, 300 mg, 0.63 mol) was combined with BCl₃ (1.9 mL, 1.9 mmol) to give Z-2 (193 mg, 79%) as a colorless oil. ¹H NMR (CDCl₃) δ 6.24 (tt, *J* = 7.5, 2.2 Hz, 1 H, C=CHCH₂CH(CH₂CH(CH₃)₂)₂), 4.21 (AB q, *J* = 11.9 Hz, 2 H, (CH₃)₂CHCH₂CO₂CH₂), 3.69 (dd, *J* = 12.1, 6.8 Hz, 1 H, CHHOH), 3.62 (dd, *J* = 12.2, 6.2 Hz, 1 H, HOCHHOH), 2.90 (dq, *J* = 16.2,

2.2 Hz, 1 H, H-3_a), 2.63–2.76 (m, 3 H, H-3_b and C=CHCH₂CH(CH₂CH(CH₃)₂)₂), 2.47 (br t, *J* = 6.3 Hz, 1 H, HOCH₂), 2.21 (d, *J* = 6.9 Hz, 2 H, (CH₃)₂CHCH₂CO₂CH₂), 2.03–2.12 (m, 1 H, (CH₃)₂CHCH₂CO₂CH₂), 1.57–1.69 (m, 3 H, C=CHCH₂CH(CH₂CH(CH₃)₂)₂), 1.08 (td, *J* = 7.0, 2.3 Hz, 4 H, C=CHCH₂CH(CH₂CH(CH₃)₂)₂), 0.94 (d, *J* = 6.6 Hz, 6 H, (CH₃)₂CHCH₂CO₂CH₂), 0.84 and 0.85 (d, *J* = 2.3 Hz, 12 H, C=CHCH₂CH(CH₂CH(CH₃)₂)₂). FAB-MS (*m/z*, relative intensity): 383 (MH⁺, 72), 57 (100). Anal. (C₂₂H₃₈O₅) C, H.

***E*-{2-(Hydroxymethyl)-4-[5-methyl-3-(2-methylpropyl)hexylidene]-5-oxo-2-(2,3-dihydrofuryl)]methyl 3-Methylbutanoate (*E*-2).** According to the general procedure, *E*-VIII (R = CH₂CH(CH₂CH(CH₃)₂), R' = CH₂CH(CH₃)₂), 103 mg, 0.22 mol) was combined with BCl₃ (0.66 mL, 0.66 mmol) to give *E*-2 (60 mg, 73%) as a colorless oil. ¹H NMR (CDCl₃) δ 6.78 (tt, *J* = 7.5, 2.8 Hz, 1 H, C=CHCH₂CH(CH₂CH(CH₃)₂)₂), 4.22 (AB q, *J* = 11.9 Hz, 2 H, (CH₃)₂CHCH₂CO₂CH₂), 3.67 (AB q, *J* = 12.1 Hz, 2 H, HOCH₂), 2.61–2.83 (m, 3 H, HOCH₂ and H-3_{a,b}), 2.20 (d, *J* = 6.8 Hz, 2 H, (CH₃)₂CHCH₂CO₂CH₂), 2.02–2.13 (m, 3 H, (CH₃)₂CHCH₂CO₂CH₂ and C=CHCH₂CH(CH₂CH(CH₃)₂)₂), 1.71 (p, *J* ≈ 6.8 Hz, 1 H, C=CHCH₂CH(CH₂CH(CH₃)₂)₂), 1.60 (sept, *J* ≈ 6.9 Hz, 2 H, C=CHCH₂CH(CH₂CH(CH₃)₂)₂), 1.05–1.12 (m, 4 H, C=CHCH₂CH(CH₂CH(CH₃)₂)₂), 0.95 (d, *J* = 6.6 Hz, 6 H, (CH₃)₂CHCH₂CO₂CH₂), 0.86 (d, *J* = 6.6 Hz, 12 H, C=CHCH₂CH(CH₂CH(CH₃)₂)₂). FAB-MS (*m/z*, relative intensity): 383 (MH⁺, 100). Anal. (C₂₂H₃₈O₅) C, H.

***Z*-[2-(Hydroxymethyl)-4-(3-methylbutylidene)-5-oxo-2-(2,3-dihydrofuryl)]methyl 5-Methyl-3-(2-methylpropyl)hexanoate (*Z*-3).** According to the general procedure, *Z*-VIII (R = CH₂CH(CH₃)₂, R' = CH₂CH(CH₂CH(CH₃)₂)₂), 127 mg, 0.27 mol) was combined with BCl₃ (0.81 mL, 0.81 mmol) to give *Z*-3 (72 mg, 67%) as a colorless oil. ¹H NMR (CDCl₃) δ 6.26 (tt, *J* = 7.8, 2.3 Hz, 1 H, C=CHCH₂CH(CH₃)₂), 4.20 (AB q, *J* = 11.9 Hz, 2 H, ((CH₃)₂CHCH₂)₂CHCH₂CO₂CH₂), 3.66 (AB q, *J* = 12.2 Hz, 2 H, HOCH₂), 2.90 (dq, *J* ≈ 16.4, 4.5, 2.2 Hz, 1 H, H-3_a), 2.72 (dq, *J* ≈ 16.4, 4.1, 2.0 Hz, 1 H, H-3_b), 2.59–2.64 (m, 2 H, C=CHCH₂CH(CH₃)₂), 2.23–2.25 (m, 2 H, ((CH₃)₂CHCH₂)₂CHCH₂CO₂CH₂), 1.89–2.02 (m, 1 H, C=CHCH₂CH(CH₃)₂), 1.68–1.78 (m, 1 H, ((CH₃)₂CHCH₂)₂CHCH₂CO₂CH₂), 1.56–1.68 (m, 2 H, ((CH₃)₂CHCH₂)₂CHCH₂CO₂CH₂), 1.02–1.20 (m, 4 H, ((CH₃)₂CHCH₂)₂CHCH₂CO₂CH₂), 0.93–0.95 (d, *J* = 6.7 Hz, 6 H, C=CHCH₂CH(CH₃)₂), 0.86–0.89 (m, 12 H, ((CH₃)₂CHCH₂)₂CHCH₂CO₂CH₂). FAB-MS (*m/z*, relative intensity): 383 (MH⁺, 100). Anal. (C₂₂H₃₈O₅) C, H.

***E*-[2-(Hydroxymethyl)-4-(3-methylbutylidene)-5-oxo-2-(2,3-dihydrofuryl)]methyl 5-Methyl-3-(2-methylpropyl)hexanoate (*E*-3).** According to the general procedure, *E*-VIII (R = CH₂CH(CH₃)₂, R' = CH₂CH(CH₂CH(CH₃)₂)₂), 260 mg, 0.56 mol) was combined with BCl₃ (1.7 mL, 1.7 mmol) to give *E*-3 (130 mg, 60%) as a pale-yellow oil. ¹H NMR (CDCl₃) δ 6.78 (tt, *J* = 7.7, 2.9 Hz, 1 H, C=CHCH₂CH(CH₃)₂), 4.21 (AB q, *J* = 11.9 Hz, 2 H, ((CH₃)₂CHCH₂)₂CHCH₂CO₂CH₂), 3.68 (AB q, *J* = 12.1 Hz, 2 H, HOCH₂), 2.82 (dm, *J* = 17.1 Hz, 1 H, H-3_a), 2.65 (dm, *J* = 17.1 Hz, 1 H, H-3_b), 2.39 (br s, 1 H, HOCH₂), 2.22–2.24 (m, 2 H, ((CH₃)₂CHCH₂)₂CHCH₂CO₂CH₂), 2.04–2.09 (m, 2 H, C=CHCH₂CH(CH₃)₂), 1.93 (app quint, 1 H, C=CHCH₂CH(CH₃)₂), 1.82 (sept, 1 H, *J* = 6.6 Hz, 1 H, ((CH₃)₂CHCH₂)₂CHCH₂CO₂CH₂), 1.60 (app sept, 2 H, ((CH₃)₂CHCH₂)₂CHCH₂CO₂CH₂), 1.03–1.18 (m, 4 H, ((CH₃)₂CHCH₂)₂CHCH₂CO₂CH₂), 0.95 (d, *J* = 6.7 Hz, 6 H, C=CHCH₂CH(CH₃)₂), 0.85–0.89 (m, 12 H, ((CH₃)₂CHCH₂)₂CHCH₂CO₂CH₂). FAB-MS (*m/z*, relative intensity): 383 (MH⁺, 100). Anal. (C₂₂H₃₈O₅) C, H.

1-({4-(Chloromethyl)-2-[(phenylmethoxy)methyl]}(1,3-dioxolan-2-yl)}methoxy)-4-methoxybenzene (X**).** 3-Chloro-1,2-propanediol (0.84 mL, 10.00 mmol) was added to a solution of **II** (1.43 g, 5.00 mmol) and *p*-TsOH·H₂O (200 mg, 1.05 mmol) in benzene (100 mL). The mixture was refluxed for 16 h with azeotropic removal of produced water. After cooling to room temperature, the mixture was diluted with EtOAc and washed sequentially with saturated NaHCO₃ and brine. The organic layer was dried over MgSO₄ and concentrated in vacuo. Purification by silica gel chromatography (hexanes/EtOAc, 15:1) gave **X** (1.29 g, 68%) as a pale-yellow oil.

¹H NMR (CDCl₃) δ 7.27–7.34 (m, 5 H, PhCH₂OCH₂), 6.81–6.88 (m, 4 H, MeOC₄H₄OCH₂), 4.60–4.61 (m, 2 H, PhCH₂OCH₂), 4.44–4.53 (m, 1 H, H-4), 4.23–4.30 (m, 1 H, MeOC₄H₄OCH₂), 3.98–4.05 (m, 3 H, MeOC₄H₄OCH₂ and H-5_{a,b}), 3.77 (s, 3 H, MeOC₄H₄OCH₂), 3.51–3.68 (m, 4 H, CHCH₂Cl and PhCH₂OCH₂). FAB-MS (*m/z*, relative intensity): 378 (M⁺, 61.3), (91, 100). Anal. (C₂₀H₂₃ClO₅) C, H.

4-Methoxy-1-({4-methylene-2-[(phenylmethoxy)methyl]}(1,3-dioxolan-2-yl)}methoxy)benzene (XI**).** A mixture of **X** (652 mg, 1.72 mmol) and ^tBuOK (386 mg, 3.44 mmol) in THF (30 mL) was refluxed for 19 h. After cooling to room temperature, the mixture was washed with water, dried over MgSO₄, and concentrated in vacuo. Purification by silica gel chromatography (hexanes/EtOAc, 15:1) gave **XI** (472 mg, 80%) as a colorless oil. ¹H NMR (CDCl₃) δ 7.27–7.32 (m, 5H, PhCH₂OCH₂), 6.81–6.90 (m, 4 H, MeOC₄H₄OCH₂), 4.62–4.63 (m, 4 H, PhCH₂OCH₂ and MeOC₄H₄OCH₂), 4.44–4.45 (m, 1 H, C=CHH), 4.10 (s, 2 H, PhCH₂OCH₂), 3.94–3.96 (m, 1 H, C=CHH), 3.77 (s, 3 H, MeOC₄H₄OCH₂), 3.72 (AB d, *J* = 1.0 Hz, 2 H, H-5_{a,b}). FAB-MS (*m/z*, relative intensity): 343 (MH⁺, 8), 91 (100). Anal. (C₂₀H₂₂O₅) C, H.

2-[(4-Methoxyphenoxy)methyl]-2-[(phenylmethoxy)methyl]-1,3-dioxolan-4-one (XII**).** **O**₃ was bubbled into a solution of **XI** (3.38 g, 9.87 mmol) in CH₂Cl₂/MeOH (20 mL/20 mL) for 10 min and then degassed with N₂ at –78 °C. To this was added dimethyl sulfide (1.45 mL, 19.7 mmol) at –78 °C, and the mixture was stirred at room temperature for 2 h. The resulting mixture was concentrated in vacuo, and the residue was dissolved in CH₂Cl₂, washed with brine, dried over MgSO₄, and concentrated in vacuo. Purification by silica gel chromatography (hexanes/EtOAc, 4:1) gave **XII** (2.42 g, 71%) as a colorless oil. ¹H NMR (CDCl₃) δ 7.29–7.38 (m, 5H, PhCH₂OCH₂), 6.80–6.86 (m, 4 H, MeOC₄H₄OCH₂), 4.63 (s, 2 H, PhCH₂OCH₂), 4.46 (AB q, *J* = 14.6 Hz, 2 H, PhCH₂OCH₂), 4.17 (AB q, *J* = 10.7 Hz, 2 H, MeOC₄H₄OCH₂), 3.80 (AB q, *J* = 11.1 Hz, H-5_{a,b}), 3.77 (s, 3 H, MeOC₄H₄OCH₂). FAB-MS (*m/z*, relative intensity): 383 (M + K⁺, 8), 344 (MH⁺, 76), 91 (100). HRMS (FAB) calcd for C₁₉H₂₀O₆ (MH⁺): 344.1260. Found: 344.1266.

2-[(4-Methoxyphenoxy)methyl]-5-(3-methylbutylidene)-2-[(phenylmethoxy)methyl]-1,3-dioxolan-4-one (XIV**, R = CH₂CH(CH₃)₂).** A solution of **XII** (1.30 g, 3.8 mmol) in THF (4 mL) was added dropwise to a solution of LDA (18 mL, 2 M in THF/hexanes, 8:1) at –78 °C. After 30 min, isovaleraldehyde (0.61 mL, 5.6 mmol) was added and the mixture was stirred at –78 °C for 2 h. The reaction was then quenched with aqueous saturated NH₄Cl, and the mixture was extracted with Et₂O (2 × 100 mL). The combined organic layer was dried over MgSO₄ and concentrated in vacuo to a yellow oil. The residual oil was then taken up in CH₂Cl₂ (30 mL) and treated sequentially with Et₃N (2.2 mL, 15.8 mmol) and MsCl (0.6 mL, 7.9 mmol) at 0 °C. After being stirred at 0 °C for 30 min, the mixture warmed to room temperature and stirred for 3 h. The mixture was then recooled to 0 °C, treated with dropwise addition of 1,8-diazabicyclo[5.4.0]undec-7-ene (DBU, 3 mL, 19.8 mmol), and allowed to warm to room temperature overnight. The mixture was then concentrated in vacuo. The residue was filtered through a short silica gel pad, washing with 50% EtOAc in hexanes, and the filtrate was concentrated in vacuo. Purification by silica gel chromatography (hexanes/EtOAc, 7:1) gave **XIV** (R = CH₂CH(CH₃)₂, 238 mg, 15%) as an equal mixture of *Z*- and *E*-isomers. ¹H NMR (CDCl₃) δ 7.28–7.37 (m, 5H, PhCH₂OCH₂), 6.79–6.85 (m, 4 H, MeOC₄H₄OCH₂), 5.67 (t, *J* = 7.9 Hz, 0.5 H, C=CHCH₂CH(CH₃)₂), 5.63 (t, *J* = 8.4 Hz, 0.5 H, C=CHCH₂CH(CH₃)₂), 4.64 (s, 2 H, PhCH₂OCH₂), 4.19 (m, 2 H, MeOC₄H₄OCH₂), 3.80–3.81 (m, 2 H, PhCH₂OCH₂), 3.77 (s, 3 H, MeOC₄H₄OCH₂), 2.40–2.53 (m, 1 H, C=CHCH₂CH(CH₃)₂), 2.09 (dd, *J* = 7.9, 6.9 Hz, 1 H, C=CHCH₂CH(CH₃)₂), 1.65–1.78 (m, 1 H, C=CHCH₂CH(CH₃)₂), 0.91–0.94 (m, 6 H, C=CHCH₂CH(CH₃)₂). FAB-MS (*m/z*, relative intensity): 412 (M⁺, 100). Anal. (C₂₄H₂₈O₆) C, H.

2-[(4-Methoxyphenoxy)methyl]-5-[5-methyl-3-(2-methylpropyl)hexylidene]-2-[(phenylmethoxy)methyl]-1,3-dioxolan-4-one (XIV**, R = CH₂CH(CH₂CH(CH₃)₂)₂).** A solution of **XII** (1.84 g, 5.34 mmol) in THF (5 mL) was added dropwise to a solution of LDA (24 mL, 2 M in THF/hexanes) at –78 °C. After 30 min, a

solution of 5-methyl-3-(2-methylpropyl)hexanal (1.82 g, 10.7 mmol) was added and the mixture was stirred at -78°C . After the mixture was stirred at -78°C for 2 h, the reaction was quenched with aqueous saturated NH_4Cl and extracted with Et_2O (2×100 mL). The combined organic layer was dried over MgSO_4 and concentrated in vacuo to a yellow oil. The residual oil was then taken up in CH_2Cl_2 (30 mL) and treated sequentially with Et_3N (3 mL, 21.4 mmol) and MsCl (1.2 mL, 16.0 mmol) at 0°C . After being stirred at 0°C for 30 min, the mixture was warmed to room temperature and stirred for 3 h. The resultant solution was then recooled to 0°C , treated with dropwise addition of DBU (8 mL, 53.4 mmol), and allowed to warm to room temperature overnight. The mixture was then concentrated in vacuo. The residue was filtered through a short silica gel pad, washing with 50% EtOAc in hexanes, and the filtrate was concentrated in vacuo. Purification by silica gel chromatography (hexanes/ EtOAc , 7:1) gave **XIV** ($\text{R} = \text{CH}_2\text{CH}(\text{CH}_2\text{CH}(\text{CH}_3)_2)$, 981 mg, 37%) as a mixture of *E*- and *Z*-isomers. $^1\text{H NMR}$ (CDCl_3) δ 7.28–7.37 (m, 5H, $\text{PhCH}_2\text{OCH}_2$), 6.79–6.85 (m, 4 H, $\text{MeOC}_4\text{H}_4\text{OCH}_2$), 5.60–5.68 (m, 1 H, $\text{C}=\text{CHCH}_2\text{CH}(\text{CH}_2\text{CH}(\text{CH}_3)_2)$), 4.64 (s, 2 H, $\text{PhCH}_2\text{OCH}_2$), 4.19 (d, $J = 6.3$ Hz, 2 H, $\text{MeOC}_4\text{H}_4\text{OCH}_2$), 3.79–3.81 (m, 2 H, $\text{PhCH}_2\text{OCH}_2$), 3.76 (s, 3 H, $\text{MeOC}_4\text{H}_4\text{OCH}_2$), 2.46–2.61 (m, 1 H, $\text{C}=\text{CHCH}_2\text{CH}(\text{CH}_2\text{CH}(\text{CH}_3)_2)$), 2.16 (dd, $J = 7.9, 5.7$ Hz, 1 H, $\text{C}=\text{CHCH}_2\text{CH}(\text{CH}_2\text{CH}(\text{CH}_3)_2)$), 1.56–1.71 (m, 3 H, $\text{C}=\text{CHCH}_2\text{CH}(\text{CH}_2\text{CH}(\text{CH}_3)_2)$), 1.06–1.11 (m, 4 H, $\text{C}=\text{CHCH}_2\text{CH}(\text{CH}_2\text{CH}(\text{CH}_3)_2)$), 0.82–0.87 (m, 12 H, $\text{C}=\text{CHCH}_2\text{CH}(\text{CH}_2\text{CH}(\text{CH}_3)_2)$). FAB-MS (m/z , relative intensity): 496 (M^+ , 56). Anal. ($\text{C}_{30}\text{H}_{40}\text{O}_6$) C, H.

2-(Hydroxymethyl)-5-(3-methylbutylidene)-2-[(phenylmethoxy)methyl]-1,3-dioxolan-4-one (XV, R = $\text{CH}_2\text{CH}(\text{CH}_3)_2$). Ammonium cerium(IV) nitrate (921 mg, 1.7 mmol) was added to a solution of **XIV** ($\text{R} = \text{CH}_2\text{CH}(\text{CH}_3)_2$, 231 mg, 0.56 mmol) in CH_3CN (16 mL) and H_2O (4 mL) at 0°C , and the mixture was stirred for 30 min. The reaction mixture was then diluted with CH_2Cl_2 and washed with H_2O . The organic layer was dried over MgSO_4 and concentrated in vacuo. Purification by silica gel chromatography (hexanes/ EtOAc , 6:1) gave **XV** ($\text{R} = \text{CH}_2\text{CH}(\text{CH}_3)_2$, 156 mg, 91%) as a yellow oil. $^1\text{H NMR}$ (CDCl_3) δ 7.28–7.37 (m, 5 H, $\text{PhCH}_2\text{OCH}_2$), 5.65 (app q, $J \approx 8.3$ Hz, 1 H, $\text{C}=\text{CHCH}_2\text{CH}(\text{CH}_3)_2$), 4.61 (s, 2 H, $\text{PhCH}_2\text{OCH}_2$), 3.82–3.84 (m, 2 H, HOCH_2), 3.67–3.74 (m, 2 H, $\text{PhCH}_2\text{OCH}_2$), 2.38–2.51 (m, ~ 1 H, $\text{C}=\text{CHCH}_2\text{CH}(\text{CH}_3)_2$), 2.10–2.14 (m, ca. 1 H, $\text{C}=\text{CHCH}_2\text{CH}(\text{CH}_3)_2$), 1.99–2.02 (br m, 1 H, HOCH_2), 1.63–1.80 (m, 1 H, $\text{C}=\text{CHCH}_2\text{CH}(\text{CH}_3)_2$), 0.90–0.94 (m, 6 H, $\text{C}=\text{CHCH}_2\text{CH}(\text{CH}_3)_2$). FAB-MS (m/z , relative intensity): 306 (M^+ , 9.7). Anal. ($\text{C}_{17}\text{H}_{22}\text{O}_5$) C, H.

2-(Hydroxymethyl)-5-[5-methyl-3-(2-methylpropyl)hexylidene]-2-[(phenylmethoxy)methyl]-1,3-dioxolan-4-one (XV, R = $\text{CH}_2\text{CH}(\text{CH}_2\text{CH}(\text{CH}_3)_2)$). Ammonium cerium(IV) nitrate (375 mg, 0.684 mmol) was added to a solution of **XIV** ($\text{R} = \text{CH}_2\text{CH}(\text{CH}_2\text{CH}(\text{CH}_3)_2)$, 113 mg, 0.228 mmol) in CH_3CN (8 mL) and H_2O (2 mL) at 0°C , and the mixture was stirred for 30 min. The reaction mixture was then diluted with CH_2Cl_2 and washed with H_2O . The organic layer was dried over MgSO_4 and concentrated in vacuo. Purification by silica gel chromatography (hexanes/ EtOAc , 6:1) gave **XV** ($\text{R} = \text{CH}_2\text{CH}(\text{CH}_2\text{CH}(\text{CH}_3)_2)$, 47 mg, 54%) as a pale-yellow oil that was not further purified and was used immediately in the following step. $^1\text{H NMR}$ (CDCl_3) δ 7.28–7.37 (m, 5H, $\text{PhCH}_2\text{OCH}_2$), 5.63 (app q, $J \approx 8.2$ Hz, 1 H, $\text{C}=\text{CHCH}_2\text{CH}(\text{CH}_2\text{CH}(\text{CH}_3)_2)$), 4.61 (2 s, 2 H, $\text{PhCH}_2\text{OCH}_2$), 3.83–3.85 (m, 2 H, HOCH_2), 3.69–3.71 (m, 2 H, $\text{PhCH}_2\text{OCH}_2$), 2.51 (m, ~ 1 H, $\text{C}=\text{CHCH}_2\text{CH}(\text{CH}_2\text{CH}(\text{CH}_3)_2)$), 2.17–2.20 (m, ca. 1 H, $\text{C}=\text{CHCH}_2\text{CH}(\text{CH}_2\text{CH}(\text{CH}_3)_2)$), 1.95 (br s, 1 H, HOCH_2), 1.55–1.57 (m, 3 H, $\text{C}=\text{CHCH}_2\text{CH}(\text{CH}_2\text{CH}(\text{CH}_3)_2)$), 1.08 (app t, 2 H, $\text{C}=\text{CHCH}_2\text{CH}(\text{CH}_2\text{CH}(\text{CH}_3)_2)$), 0.84–0.86 (m, 12 H, $\text{C}=\text{CHCH}_2\text{CH}(\text{CH}_2\text{CH}(\text{CH}_3)_2)$).

{5-[5-Methyl-3-(2-methylpropyl)hexylidene]-4-oxo-2-[(phenylmethoxy)methyl]-1,3-dioxolan-2-yl}methyl 5-Methyl-3-(2-methylpropyl)hexanoate (XVI, R = $\text{CH}_2\text{CH}(\text{CH}_3)_2$, R' = $\text{CH}_2\text{CH}(\text{CH}_2\text{CH}(\text{CH}_3)_2)$). Et_3N (0.14 mL, 1.02 mmol) and 5-methyl-3-(2-methylpropyl)hexanoyl chloride (0.02 mL, 0.16 mmol) were added sequentially to a 0°C stirring solution of **XV** ($\text{R} = \text{CH}_2\text{CH}(\text{CH}_3)_2$) (156 mg, 0.51 mmol) in CH_2Cl_2 (20 mL). After the mixture was allowed to warm to room temperature and was stirred for 4 h, the mixture was washed with

aqueous saturated NaHCO_3 ($1 \times$), dried over MgSO_4 , and concentrated in vacuo. Purification by silica gel chromatography (hexanes/ EtOAc , 20:1) gave an equal mixture of geometric isomers **XVI** ($\text{R} = \text{CH}_2\text{CH}(\text{CH}_3)_2$, R' = $\text{CH}_2\text{CH}(\text{CH}_2\text{CH}(\text{CH}_3)_2)$, 114 mg, 46%) as a yellow oil. $^1\text{H NMR}$ (CDCl_3) δ 7.28–7.37 (m, 5H, $\text{PhCH}_2\text{OCH}_2$), 5.66 (t, $J = 8.0$ Hz, 0.5 H, $\text{C}=\text{CHCH}_2\text{CH}(\text{CH}_3)_2$), 5.62 (t, $J = 8.5$ Hz, 0.5 H, $\text{C}=\text{CHCH}_2\text{CH}(\text{CH}_3)_2$), 4.61 (s, 2 H, $\text{PhCH}_2\text{OCH}_2$), 4.29–4.39 (m, 2 H, $((\text{CH}_3)_2\text{CHCH}_2)_2\text{CHCH}_2\text{CO}_2\text{CH}_2$), 3.65–3.72 (m, 2 H, $\text{PhCH}_2\text{OCH}_2$), 2.37–2.51 (m, ~ 1 H, $\text{C}=\text{CHCH}_2\text{CH}(\text{CH}_3)_2$), 2.20–2.26 (m, ~ 1 H, $((\text{CH}_3)_2\text{CHCH}_2)_2\text{CHCH}_2\text{CO}_2\text{CH}_2$), 2.08–2.11 (app t, 1 H, $((\text{CH}_3)_2\text{CHCH}_2)_2\text{CHCH}_2\text{CO}_2\text{CH}_2$), 1.89–1.99 (m, 1 H, $\text{C}=\text{CHCH}_2\text{CH}(\text{CH}_3)_2$), 1.54–1.79 (m, 3 H, $((\text{CH}_3)_2\text{CHCH}_2)_2\text{CHCH}_2\text{CO}_2\text{CH}_2$), 1.02–1.17 (m, 4 H, $((\text{CH}_3)_2\text{CHCH}_2)_2\text{CHCH}_2\text{CO}_2\text{CH}_2$), 0.85–0.93 (18 H, $\text{C}=\text{CHCH}_2\text{CH}(\text{CH}_3)_2$ and $((\text{CH}_3)_2\text{CHCH}_2)_2\text{CHCH}_2\text{CO}_2\text{CH}_2$). FAB-MS (m/z , relative intensity): 475 (MH^+ , 2), (91, 100). Anal. ($\text{C}_{28}\text{H}_{42}\text{O}_6$) C, H.

{5-[5-Methyl-3-(2-methylpropyl)hexylidene]-4-oxo-2-[(phenylmethoxy)methyl]-1,3-dioxolan-2-yl}methyl 2,2-Dimethylpropanoate (XVI, R = $\text{CH}_2\text{CH}(\text{CH}_2\text{CH}(\text{CH}_3)_2)$, R' = $\text{C}(\text{CH}_3)_3$). DMAP (2 mg, 0.013 mmol), Et_3N (0.04 mL, 0.26 mmol), and pivaloyl chloride (0.02 mL, 0.16 mmol) were added sequentially to a 0°C solution of **XV** ($\text{R} = \text{CH}_2\text{CH}(\text{CH}_2\text{CH}(\text{CH}_3)_2)$, 51 mg, 0.13 mmol) in CH_2Cl_2 (5 mL). After being stirred for 2 h, the mixture was washed with aqueous saturated NaHCO_3 ($1 \times$) and brine ($1 \times$), dried over MgSO_4 , and concentrated in vacuo. Purification by silica gel chromatography (hexanes/ EtOAc 20:1) gave **XVI** ($\text{R} = \text{CH}_2\text{CH}(\text{CH}_2\text{CH}(\text{CH}_3)_2)$, R' = $\text{C}(\text{CH}_3)_3$, 51 mg, 82%) as a colorless oil that was used without further purification in the next step. $^1\text{H NMR}$ (CDCl_3) δ 7.28–7.37 (m, 5 H, $\text{PhCH}_2\text{OCH}_2$), 5.65 (t, $J = 7.8$ Hz, 0.5 H, $\text{C}=\text{CHCH}_2\text{CH}(\text{CH}_2\text{CH}(\text{CH}_3)_2)$), 5.62 (t, $J = 8.3$ Hz, 0.5 H, $\text{C}=\text{CHCH}_2\text{CH}(\text{CH}_2\text{CH}(\text{CH}_3)_2)$), 4.62 (s, 2 H, $\text{PhCH}_2\text{OCH}_2$), 4.37 (AB q, $J = 12.3$ Hz, 1 H, $\text{CH}_3\text{C}(\text{O})\text{OCH}_2$), 4.34 (s, 1 H, $\text{CH}_3\text{C}(\text{O})\text{OCH}_2$), 3.67–3.69 (m, 2 H, $\text{PhCH}_2\text{OCH}_2$), 2.49–2.53 (m, 1 H, $\text{C}=\text{CHCH}_2\text{CH}(\text{CH}_2\text{CH}(\text{CH}_3)_2)$), 2.15–2.19 (m, 1 H, $\text{C}=\text{CHCH}_2\text{CH}(\text{CH}_2\text{CH}(\text{CH}_3)_2)$), 1.54–1.71 (m, 3 H, $\text{C}=\text{CHCH}_2\text{CH}(\text{CH}_2\text{CH}(\text{CH}_3)_2)$), 1.17 and 1.18 (s, 9 H, $\text{CH}_3\text{C}(\text{O})\text{OCH}_2$), 1.08 (td, $J = 7.0, 2.2$ Hz, 4 H, $\text{C}=\text{CHCH}_2\text{CH}(\text{CH}_2\text{CH}(\text{CH}_3)_2)$), 0.84–0.86 (m, 12 H, $\text{C}=\text{CHCH}_2\text{CH}(\text{CH}_2\text{CH}(\text{CH}_3)_2)$). FAB-MS (m/z , relative intensity): 513 (MH^+ , 8), 475 (MH^+ , 2), 91 (100).

{5-[5-Methyl-3-(2-methylpropyl)hexylidene]-4-oxo-2-[(phenylmethoxy)methyl]-1,3-dioxolan-2-yl}methyl 3-Methylbutanoate (XVI, R = $\text{CH}_2\text{CH}(\text{CH}_2\text{CH}(\text{CH}_3)_2)$, R' = $\text{CH}_2\text{CH}(\text{CH}_3)_2$). Isovaleryl chloride (0.05 mL, 0.41 mmol) was added dropwise to a 0°C stirring solution of DMAP (5 mg, 0.034 mmol), pyridine (0.05 mL, 0.68 mmol), and **XV** ($\text{R} = \text{CH}_2\text{CH}(\text{CH}_2\text{CH}(\text{CH}_3)_2)$) in CH_2Cl_2 (10 mL). The ice bath was removed and the reaction mixture warmed to room temperature. After being stirred at room temperature for 24 h, the mixture was washed with aqueous saturated NaHCO_3 ($1 \times$) and brine ($1 \times$), dried over MgSO_4 , and concentrated in vacuo. Purification by silica gel chromatography gave **XVI** ($\text{R} = \text{CH}_2\text{CH}(\text{CH}_2\text{CH}(\text{CH}_3)_2)$, R' = $\text{CH}_2\text{CH}(\text{CH}_3)_2$, 135 mg, 84%) as a pale-yellow oil consisting of predominantly a single isomer. $^1\text{H NMR}$ (CDCl_3) δ 7.29–7.38 (m, 5H, $\text{PhCH}_2\text{OCH}_2$), 5.65 (t, $J = 7.9$ Hz, 1 H, $\text{C}=\text{CHCH}_2\text{CH}(\text{CH}_2\text{CH}(\text{CH}_3)_2)$), 4.61 (s, 2 H, $\text{PhCH}_2\text{OCH}_2$), 4.30 (AB q, $J = 12.3$ Hz, 2 H, $\text{PhCH}_2\text{OCH}_2$), $\text{PhCH}_2\text{OCH}_2$), 3.65–3.71 (m, 2 H, $(\text{CH}_3)_2\text{CHCH}_2\text{CO}_2\text{CH}_2$), 2.15–2.21 (m, 4 H, $\text{C}=\text{CHCH}_2\text{CH}(\text{CH}_2\text{CH}(\text{CH}_3)_2)$ and $(\text{CH}_3)_2\text{CHCH}_2\text{CO}_2\text{CH}_2$), 2.00–2.10 (m, 1 H, $(\text{CH}_3)_2\text{CHCH}_2\text{CO}_2\text{CH}_2$), 1.57–1.71 (m, 3 H, $\text{C}=\text{CHCH}_2\text{CH}(\text{CH}_2\text{CH}(\text{CH}_3)_2)$), 1.08 (td, $J = 7.1, 1.4$ Hz, 1 H, $\text{C}=\text{CHCH}_2\text{CH}(\text{CH}_2\text{CH}(\text{CH}_3)_2)$), 0.93 and 0.94 (s, 6 H, $(\text{CH}_3)_2\text{CHCH}_2\text{CO}_2\text{CH}_2$), 0.84 and 0.86 (s, 12 H, $\text{C}=\text{CHCH}_2\text{CH}(\text{CH}_2\text{CH}(\text{CH}_3)_2)$). FAB-MS (m/z , relative intensity): 475 (MH^+ , 2), (91, 100). Anal. ($\text{C}_{28}\text{H}_{42}\text{O}_6$) C, H

{2-(Hydroxymethyl)-5-[5-methyl-3-(2-methylpropyl)hexylidene]-4-oxo-1,3-dioxolan-2-yl}methyl 2,2-Dimethylpropanoate (Z,E-4). BCl_3 (0.3 mL, 0.32 mmol, 1 M in CH_2Cl_2) was added to a -78°C solution of **XVI** ($\text{R} = \text{CH}_2\text{CH}(\text{CH}_2\text{CH}(\text{CH}_3)_2)$, R' = $\text{C}(\text{CH}_3)_3$, 51 mg, 0.11 mmol) in CH_2Cl_2 (5 mL), and the mixture was stirred for 2 h. The reaction was quenched with aqueous saturated NaHCO_3 , extracted with CH_2Cl_2 ($2 \times$), dried over MgSO_4 , and

concentrated in vacuo. Purification by silica gel chromatography (hexanes/EtOAc, 6:1) gave *Z,E*-4 (35.2 mg, 86% as a 1:1 mixture of geometric isomers) as a pale-yellow oil. $^1\text{H NMR}$ (CDCl_3) δ 5.67 (t, $J = 7.9$ Hz, 0.5 H, $\text{C}=\text{CHCH}_2\text{CH}(\text{CH}_2\text{CH}(\text{CH}_3)_2)_2$), 5.64 (t, $J = 8.3$ Hz, 0.5 H, $\text{C}=\text{CHCH}_2\text{CH}(\text{CH}_2\text{CH}(\text{CH}_3)_2)_2$), 4.29–4.41 (m, 2 H, $\text{CH}_3\text{C}(\text{O})\text{OCH}_2$), 3.80 (br t, 2 H, HOCH_2), 2.50 (dd, $J = 8.3, 6.0$ Hz, 1 H, $\text{C}=\text{CHCH}_2\text{CH}(\text{CH}_2\text{CH}(\text{CH}_3)_2)_2$), 2.17 (dd, $J = 7.8, 5.8$ Hz, 1 H, $\text{C}=\text{CHCH}_2\text{CH}(\text{CH}_2\text{CH}(\text{CH}_3)_2)_2$), 2.14 (v br s, 1 H, HOCH_2), 1.55–1.70 (m, 3 H, $\text{C}=\text{CHCH}_2\text{CH}(\text{CH}_2\text{CH}(\text{CH}_3)_2)_2$), 1.18 and 1.19 (s, 9 H, $\text{OC}(\text{O})\text{CH}_3$), 1.06–1.10 (m, 4 H, $\text{C}=\text{CHCH}_2\text{CH}(\text{CH}_2\text{CH}(\text{CH}_3)_2)_2$), 0.84–0.87 (m, 12 H, $\text{C}=\text{CHCH}_2\text{CH}(\text{CH}_2\text{CH}(\text{CH}_3)_2)_2$). FAB-MS (m/z , relative intensity): 385 (MH^+ , 23), (57, 100). Anal. ($\text{C}_{21}\text{H}_{36}\text{O}_6$) C, H.

[2-(Hydroxymethyl)-5-[5-methyl-3-(2-methylpropyl)hexylidene]-4-oxo-1,3-dioxolan-2-yl]methyl 3-Methylbutanoate (*Z,E*-5). BCl_3 (1.4 mL, 1.4 mmol, 1 M in CH_2Cl_2) was added to a -78 °C solution of **XVI** ($\text{R} = \text{CH}_2\text{CH}(\text{CH}_2\text{CH}(\text{CH}_3)_2)_2$, $\text{R}' = \text{CH}_2\text{CH}(\text{CH}_3)_2$, 135 mg, 0.28 mmol) in CH_2Cl_2 (10 mL), and the mixture was stirred for 2 h. The reaction was quenched with aqueous saturated NaHCO_3 , extracted with CH_2Cl_2 (2 \times), dried over MgSO_4 , and concentrated in vacuo. Purification by silica gel chromatography (hexanes/EtOAc, 5:1) gave *Z,E*-5 (87 mg, 80% as a single geometric isomer) as a pale-yellow oil that solidified upon standing: mp 50–51 °C; $^1\text{H NMR}$ (CDCl_3) δ 5.68 (t, $J = 7.9$ Hz, 1 H, $\text{C}=\text{CHCH}_2\text{CH}(\text{CH}_3)_2$), 4.36 (AB q, $J = 12.4$ Hz, 2 H, $((\text{CH}_3)_2\text{CHCH}_2\text{CO}_2\text{CH}_2)$), 3.82 (br AB d, 2 H, HOCH_2), 2.21–2.23 (m, 2 H, $(\text{CH}_3)_2\text{CHCH}_2\text{CO}_2\text{CH}_2$), 2.17 (dd, $J = 7.9, 5.7$ Hz, 2 H, $\text{C}=\text{CHCH}_2\text{CH}(\text{CH}_2\text{CH}(\text{CH}_3)_2)_2$), 2.07 (p, $J = 6.7$ Hz, 1 H, $(\text{CH}_3)_2\text{CHCH}_2\text{CO}_2\text{CH}_2$), 1.98 (v br t, 1 H, HOCH_2), 1.57–1.72 (m, 3 H, $\text{C}=\text{CHCH}_2\text{CH}(\text{CH}_2\text{CH}(\text{CH}_3)_2)_2$), 1.09 (br t, $J = 7.0$ Hz, 4 H, $\text{C}=\text{CHCH}_2\text{CH}(\text{CH}_2\text{CH}(\text{CH}_3)_2)_2$), 0.95 (d, $J = 6.7$ Hz, 6 H, $(\text{CH}_3)_2\text{CHCH}_2\text{CO}_2\text{CH}_2$), 0.85–0.87 (m, 12 H, $\text{C}=\text{CHCH}_2\text{CH}(\text{CH}_2\text{CH}(\text{CH}_3)_2)_2$). FAB-MS (m/z , relative intensity): 385 (MH^+ , 18), 85 (100). Anal. ($\text{C}_{21}\text{H}_{36}\text{O}_6$) C, H.

[2-(Hydroxymethyl)-5-(3-methylbutylidene)-4-oxo-1,3-dioxolan-2-yl]methyl 5-Methyl-3-(2-methylpropyl)hexanoate (*Z,E*-6). BCl_3 (1.2 mL, 1.1 mmol, 1 M in CH_2Cl_2) was added to a -78 °C solution of **XVI** ($\text{R} = \text{CH}_2\text{CH}(\text{CH}_3)_2$, $\text{R}' = \text{CH}_2\text{CH}(\text{CH}_2\text{CH}(\text{CH}_3)_2)_2$, 107 mg, 0.23 mmol) in CH_2Cl_2 (10 mL), and the mixture was stirred for 2 h. The reaction was quenched with aqueous saturated NaHCO_3 , extracted with CH_2Cl_2 (2 \times), dried over MgSO_4 , and concentrated in vacuo. Purification by silica gel chromatography (hexanes/EtOAc, 6:1) gave *Z,E*-6 (52 mg, 60% as a 3:2 mixture of geometric isomers) as a pale-yellow oil. $^1\text{H NMR}$ (CDCl_3) δ 5.69 (t, $J = 8.0$ Hz, 0.6 H, $\text{C}=\text{CHCH}_2\text{CH}(\text{CH}_3)_2$), 5.66 (t, $J = 8.6$ Hz, 0.4 H, $\text{C}=\text{CHCH}_2\text{CH}(\text{CH}_3)_2$), 4.34 (s, 0.6 H, $((\text{CH}_3)_2\text{CHCH}_2)_2\text{CHCH}_2\text{CO}_2\text{CH}_2$), 4.32 (AB q, $J = 12.4$ Hz, 0.4 H, $((\text{CH}_3)_2\text{CHCH}_2)_2\text{CHCH}_2\text{CO}_2\text{CH}_2$), 3.82 (AB q, $J = 12.8$ Hz, 0.6 H, HOCH_2), 3.80 (s, 0.4 Hz, 0.4 H, HOCH_2), 2.45 (dd, $J = 8.6, 6.8$ Hz, 1 H, $\text{C}=\text{CHCH}_2\text{CH}(\text{CH}_3)_2$), 2.23–2.26 (m, 2 H, $((\text{CH}_3)_2\text{CHCH}_2)_2\text{CHCH}_2\text{CO}_2\text{CH}_2$), 2.11 (dd, $J = 7.9, 6.9$ Hz, 1 H, $\text{C}=\text{CHCH}_2\text{CH}(\text{CH}_3)_2$), 1.90–1.99 (m, 1 H, $\text{C}=\text{CHCH}_2\text{CH}(\text{CH}_3)_2$), 1.53–1.81 (m, 3 H, $((\text{CH}_3)_2\text{CHCH}_2)_2\text{CHCH}_2\text{CO}_2\text{CH}_2$), 1.03–1.18 (m, 4 H, $((\text{CH}_3)_2\text{CHCH}_2)_2\text{CHCH}_2\text{CO}_2\text{CH}_2$), 0.93 (d, $J = 6.6$ Hz, 6 H, $\text{C}=\text{CHCH}_2\text{CH}(\text{CH}_3)_2$), 0.86–0.89 (m, 12 H, $((\text{CH}_3)_2\text{CHCH}_2)_2\text{CHCH}_2\text{CO}_2\text{CH}_2$). FAB-MS (m/z , relative intensity): 385 (MH^+ , 100), Anal. ($\text{C}_{21}\text{H}_{36}\text{O}_6$) C, H.

Acknowledgment. This research was supported by the Intramural Research Program of the NIH, National Cancer Institute, Center for Cancer Research. The authors thank Dr. James A. Kelley from the Laboratory of Medicinal Chemistry for mass spectral analysis and interpretation. This research has been funded in part with federal funds from the National Cancer Institute, National Institutes of Health, under Contract N01-CO-12400. The content of this publication does not necessarily reflect the views or policies of the Department of Health and Human Services nor does mention of trade names, commercial products, or organizations imply endorsement by the U.S. Government.

Supporting Information Available: $^1\text{H NMR}$ spectra and combustion analysis results. This material is available free of charge via the Internet at <http://pubs.acs.org>.

References

- Nishizuka, Y. Intracellular signaling by hydrolysis of phospholipids and activation of protein-kinase-C. *Science* **1992**, *258*, 607–614.
- Hofmann, J. Protein kinase C isozymes as potential targets for anticancer therapy. *Curr. Cancer Drug. Targets* **2004**, *4*, 125–146.
- Garcia-Bermejo, M. L.; Leskow, F. C.; Fujii, T.; Wang, Q.; Blumberg, P. M.; Ohba, M.; Kuroki, T.; Han, K. C.; Lee, J.; Marquez, V. E.; Kazanietz, M. G. Diacylglycerol (DAG)-lactones, a new class of protein kinase C (PKC) agonists, induce apoptosis in LNCaP prostate cancer cells by selective activation of PKC α . *J. Biol. Chem.* **2002**, *277*, 645–655.
- Mochly-Rosen, D.; Kauvar, L. M. Pharmacological regulation of network kinetics by protein kinase C localization. *Semin. Immunol.* **2000**, *12*, 55–61.
- Newton, A. C. Protein kinase C: structural and spatial regulation by phosphorylation, cofactors, and macromolecular interactions. *Chem. Rev.* **2001**, *101*, 2353–2364.
- Parker, P. J.; Murray-Rust, J. PKC at a glance. *J. Cell Sci.* **2004**, *117*, 131–132.
- Ono, Y.; Fujii, T.; Igarashi, K.; Kuno, T.; Tanaka, C.; Kikkawa, U.; Nishizuka, Y. Phorbol ester binding to protein kinase-C requires a cysteine-rich zinc-finger-like sequence. *Proc. Natl. Acad. Sci. U.S.A.* **1989**, *86*, 4868–4871.
- Ron, D.; Kazanietz, M. G. New insights into the regulation of protein kinase C and novel phorbol ester receptors. *FASEB J.* **1999**, *13*, 1658–1676.
- Rozengurt, E.; Sinnett-Smith, J.; Zugaza, J. Protein kinase D: a novel target for diacylglycerol and phorbol esters. *Biochem. Soc. Trans.* **1997**, *25*, 565–571.
- Ahmed, S.; Lee, J.; Kozma, R.; Best, A.; Monfries, C.; Lim, L. A novel functional target for tumor-promoting phorbol esters and lysophosphatidic acid. The P21rac-Gtpase activating protein *N-chimaerin*. *J. Biol. Chem.* **1993**, *268*, 10709–10712.
- Brose, N.; Rosenmund, C.; Rettig, J. Regulation of transmitter release by Unc-13 and its homologues. *Curr. Opin. Neurobiol.* **2000**, *10*, 303–311.
- Ebinu, J. O.; Bottorff, D. A.; Chan, E. Y. W.; Stang, S. L.; Dunn, R. J.; Stone, J. C. RasGRP, a Ras guanyl nucleotide-releasing protein with calcium- and diacylglycerol-binding motifs. *Science* **1998**, *280*, 1082–1086.
- Kawasaki, H.; Sprightgett, G. M.; Toki, S.; Canales, J. J.; Harlan, P.; Blumenstiel, J. P.; Chen, E. J.; Bany, I. A.; Mochizuki, N.; Ashbacher, A.; Matsuda, M.; Housman, D. E.; Graybiel, A. M. A Rap guanine nucleotide exchange factor enriched highly in the basal ganglia. *Proc. Natl. Acad. Sci. U.S.A.* **1998**, *95*, 13278–13283.
- Luo, B.; Regier, D. S.; Prescott, S. M.; Topham, M. K. Diacylglycerol kinases. *Cell. Signalling* **2004**, *16*, 983–989.
- van Blitterswijk, W. J.; Houssa, B. Properties and functions of diacylglycerol kinases. *Cell. Signalling* **2000**, *12*, 595–605.
- Zhang, G. G.; Kazanietz, M. G.; Blumberg, P. M.; Hurley, J. H. Crystal-structure of the Cys2 activator-binding domain of protein-kinase C-Delta in complex with phorbol ester. *Cell* **1995**, *81*, 917–924.
- Marquez, V. E.; Blumberg, P. M. Synthetic diacylglycerols (DAG) and DAG-lactones as activators of protein kinase C (PK-C). *Acc. Chem. Res.* **2003**, *36*, 434–443.
- Hamer, D. H.; Bocklandt, S.; McHugh, L.; Chun, T. W.; Blumberg, P. M.; Sigano, D. M.; Marquez, V. E. Rational design of drugs that induce human immunodeficiency virus replication. *J. Virol.* **2003**, *77*, 10227–10236.
- Pu, Y.; Perry, N. A.; Yang, D.; Lewin, N. E.; Kedei, N.; Braun, D. C.; Choi, S. H.; Blumberg, P. M.; Garfield, S. H.; Stone, J. C.; Duan, D.; Marquez, V. E. A novel diacylglycerol-lactone shows marked selectivity in vitro among C1 domains of protein kinase C (PKC) isoforms alpha and delta as well as selectivity for RasGRP compared with PKC α . *J. Biol. Chem.* **2005**, *280*, 27329–27338.
- Lee, J. Design and synthesis of bioisosteres of ultrapotent protein kinase C (PKC) ligand, 5-acetoxymethyl-5-hydroxymethyl-3-alkylidene tetrahydro-2-furanone. *Arch. Pharmacol. Res.* **1998**, *21*, 452–457.
- Choi, Y.; Kang, J. H.; Lewin, N. E.; Blumberg, P. M.; Lee, J.; Marquez, V. E. Conformationally constrained analogues of diacylglycerol. 19. Synthesis and protein kinase C binding affinity of diacylglycerol lactones bearing an *N*-hydroxylamide side chain. *J. Med. Chem.* **2003**, *46*, 2790–2793.

- (22) Kang, J. H.; Benzaria, S.; Sigano, D. M.; Lewin, N. E.; Pu, Y. M.; Peach, M. L.; Blumberg, P. M.; Marquez, V. E. Conformationally constrained analogues of diacylglycerol. 26. Exploring the chemical space surrounding the C1 domain of protein kinase C with DAG-lactones containing aryl groups at the sn-1 and sn-2 positions. *J. Med. Chem.* **2006**, *49*, 3185–3203.
- (23) Wildman, S. A.; Crippen, G. M. Prediction of physicochemical parameters by atomic contributions. *J. Chem. Inf. Comput. Sci.* **1999**, *39*, 868–873.
- (24) Lee, J.; Han, K. C.; Kang, J. H.; Pearce, L. L.; Lewin, N. E.; Yan, S.; Benzaria, S.; Nicklaus, M. C.; Blumberg, P. M.; Marquez, V. E. Conformationally constrained analogues of diacylglycerol. 18. The incorporation of a hydroxamate moiety into diacylglycerol-lactones reduces lipophilicity and helps discriminate between sn-1 and sn-2 binding modes to protein kinase C (PK-C). Implications for isozyme specificity. *J. Med. Chem.* **2001**, *44*, 4309–4312. Erratum: *J. Med. Chem.* **2003**, *46* (13), 2794.
- (25) Kang, J. H.; Peach, M. L.; Pu, Y. M.; Lewin, N. E.; Nicklaus, M. C.; Blumberg, P. M.; Marquez, V. E. Conformationally constrained analogues of diacylglycerol (DAG). 25. Exploration of the sn-1 and sn-2 carbonyl functionality reveals the essential role of the sn-1 carbonyl at the lipid interface in the binding of DAG-lactones to protein kinase C. *J. Med. Chem.* **2005**, *48*, 5738–5748.
- (26) Sigano, D. M.; Peach, M. L.; Nacro, K.; Choi, Y.; Lewin, N. E.; Nicklaus, M. C.; Blumberg, P. M.; Marquez, V. E. Differential binding modes of diacylglycerol (DAG) and DAG lactones to protein kinase C (PK-C). *J. Med. Chem.* **2003**, *46*, 1571–1579.
- (27) Kazanietz, M. G.; Wang, S.; Milne, G. W.; Lewin, N. E.; Liu, H. L.; Blumberg, P. M. Residues in the second cysteine-rich region of protein kinase C delta relevant to phorbol ester binding as revealed by site-directed mutagenesis. *J. Biol. Chem.* **1995**, *270*, 21852–21859.
- (28) Irie, K.; Nakahara, A.; Nakagawa, Y.; Ohigashi, H.; Shindo, M.; Fukuda, H.; Konishi, H.; Kikkawa, U.; Kashiwagi, K.; Saito, N. Establishment of a binding assay for protein kinase C isozymes using synthetic C1 peptides and development of new medicinal leads with protein kinase C isozyme and C1 domain selectivity. *Pharmacol. Ther.* **2002**, *93*, 271–281.
- (29) Im, W.; Feig, M.; Brooks, C. L., III. An implicit membrane generalized Born theory for the study of structure, stability, and interactions of membrane proteins. *Biophys. J.* **2003**, *85*, 2900–2918.
- (30) Bogi, K.; Lorenzo, P. S.; Szallasi, Z.; Acs, P.; Wagner, G. S.; Blumberg, P. M. Differential selectivity of ligands for the C1A and C1B phorbol ester binding domains of protein kinase C delta: Possible correlation with tumor-promoting activity. *Cancer Res.* **1998**, *58*, 1423–1428.
- (31) Yang, C. F.; Kazanietz, M. G. Divergence and complexities in DAG signaling: looking beyond PKC. *Trends Pharmacol. Sci.* **2003**, *24*, 602–608.
- (32) Goekjian, P. G.; Jirousek, M. R. Protein kinase C in the treatment of disease: signal transduction pathways, inhibitors, and agents in development. *Curr. Med. Chem.* **1999**, *6*, 877–903.
- (33) Meier, M.; King, G. L. Protein kinase C activation and its pharmacological inhibition in vascular disease. *Vasc. Med.* **2000**, *5*, 173–185.
- (34) Tortora, G.; Ciardiello, F. Antisense strategies targeting protein kinase C: preclinical and clinical development. *Semin. Oncol.* **2003**, *30*, 26–31.
- (35) Szallasi, Z.; Denning, M. F.; Smith, C. B.; Dlugosz, A. A.; Yuspa, S. H.; Pettit, G. R.; Blumberg, P. M. Bryostatin 1 protects protein kinase C-delta from down-regulation in mouse keratinocytes in parallel with its inhibition of phorbol ester-induced differentiation. *Mol. Pharmacol.* **1994**, *46*, 840–850.
- (36) Szallasi, Z.; Smith, C. B.; Pettit, G. R.; Blumberg, P. M. Differential regulation of protein kinase C isozymes by bryostatin 1 and phorbol 12-myristate 13-acetate in NIH 3T3 fibroblasts. *J. Biol. Chem.* **1994**, *269*, 2118–2124.
- (37) Szallasi, Z.; Krsmanovic, L.; Blumberg, P. M. Nonpromoting 12-deoxyphorbol 13-esters inhibit phorbol 12-myristate 13-acetate induced tumor promotion in Cd-1 mouse skin. *Cancer Res.* **1993**, *53*, 2507–2512.
- (38) Bocklandt, S.; Blumberg, P. M.; Hamer, D. H. Activation of latent HIV-1 expression by the potent anti-tumor promoter 12-deoxyphorbol 13-phenylacetate. *Antiviral Res.* **2003**, *59*, 89–98.
- (39) Kedei, N.; Lundberg, D. J.; Toth, A.; Welburn, P.; Garfield, S. H.; Blumberg, P. M. Characterization of the interaction of ingenol 3-angelate with protein kinase C. *Cancer Res.* **2004**, *64*, 3243–3255.
- (40) Hommel, U.; Zurini, M.; Luyten, M. Solution structure of a cysteine-rich domain of rat protein-kinase-C. *Nat. Struct. Biol.* **1994**, *1*, 383–387.
- (41) Hritz, J.; Ulicny, J.; Laaksonen, A.; Jancura, D.; Miskovsky, P. Molecular interaction model for the C1B domain of protein kinase C-gamma in the complex with its activator phorbol-12-myristate-13-acetate in water solution and lipid bilayer. *J. Med. Chem.* **2004**, *47*, 6547–6555.
- (42) Burns, D. J.; Bell, R. M. Protein-kinase-C contains 2 phorbol ester binding domains. *J. Biol. Chem.* **1991**, *266*, 18330–18338.
- (43) Zhu, J. W.; Hansen, H.; Su, L. H.; Shieh, H. L.; Riedel, H. Ligand regulation of bovine protein-kinase-C-alpha response via either cysteine-rich repeat of conserved region C1. *J. Biochem.* **1994**, *115*, 1000–1009.
- (44) Medkova, M.; Cho, W. H. Interplay of C1 and C2 domains of protein kinase C-alpha in its membrane binding and activation. *J. Biol. Chem.* **1999**, *274*, 19852–19861.
- (45) Giorgione, J.; Hysell, M.; Harvey, D. F.; Newton, A. C. Contribution of the C1A and C1B domains to the membrane interaction of protein kinase C. *Biochemistry* **2003**, *42*, 11194–11202.
- (46) Irie, K.; Nakagawa, Y.; Ohigashi, H. Indolactam and benzolactam compounds as new medicinal leads with binding selectivity for C1 domains of protein kinase C isozymes. *Curr. Pharm. Des.* **2004**, *10*, 1371–1385.
- (47) Irie, K.; Nakagawa, Y.; Ohigashi, H. Toward the development of new medicinal leads with selectivity for protein kinase C isozymes. *Chem. Rec.* **2005**, *5*, 185–195.
- (48) Lorenzo, P. S.; Bogi, K.; Hughes, K. M.; Beheshti, M.; Bhattacharyya, D.; Garfield, S. H.; Pettit, G. R.; Blumberg, P. M. Differential roles of the tandem C1 domains of protein kinase C delta in the biphasic down-regulation induced by bryostatin 1. *Cancer Res.* **1999**, *59*, 6137–6144.
- (49) Szallasi, Z.; Bogi, K.; Gohari, S.; Biro, T.; Acs, P.; Blumberg, P. M. Non-equivalent roles for the first and second zinc fingers of protein kinase Cdelta. Effect of their mutation on phorbol ester-induced translocation in NIH 3T3 cells. *J. Biol. Chem.* **1996**, *271*, 18299–18301.
- (50) Stahelin, R. V.; Digman, M. A.; Medkova, M.; Ananthanarayanan, B.; Rafter, J. D.; Melowic, H. R.; Cho, W. H. Mechanism of diacylglycerol-induced membrane targeting and activation of protein kinase C delta. *J. Biol. Chem.* **2004**, *279*, 29501–29512.
- (51) Kazanietz, M. G.; Arecas, L. B.; Bahador, A.; Mischak, H.; Goodnight, J.; Mushinski, J. F.; Blumberg, P. M. Characterization of ligand and substrate specificity for the calcium-dependent and calcium-independent protein kinase C isozymes. *Mol. Pharmacol.* **1993**, *44*, 298–307.
- (52) Lewin, N. E.; Blumberg, P. M. [³H]Phorbol 12,13-dibutyrate binding assay for protein kinase C and related proteins. *Methods Mol. Biol.* **2003**, *233*, 129–156.
- (53) Sharma, R.; Lee, J.; Wang, S.; Milne, G. W.; Lewin, N. E.; Blumberg, P. M.; Marquez, V. E. Conformationally constrained analogues of diacylglycerol. 10. Ultrapotent protein kinase C ligands based on a racemic 5-disubstituted tetrahydro-2-furanone template. *J. Med. Chem.* **1996**, *39*, 19–28.
- (54) Lee, J.; Wang, S.; Milne, G. W.; Sharma, R.; Lewin, N. E.; Blumberg, P. M.; Marquez, V. E. Conformationally constrained analogues of diacylglycerol. 11. Ultrapotent protein kinase C ligands based on a chiral 5-disubstituted tetrahydro-2-furanone template. *J. Med. Chem.* **1996**, *39*, 29–35.
- (55) Lee, J.; Sharma, R.; Wang, S.; Milne, G. W.; Lewin, N. E.; Szallasi, Z.; Blumberg, P. M.; George, C.; Marquez, V. E. Conformationally constrained analogues of diacylglycerol. 12. Ultrapotent protein kinase C ligands based on a chiral 4,4-disubstituted heptono-1,4-lactone template. *J. Med. Chem.* **1996**, *39*, 36–45.
- (56) Teng, K.; Marquez, V. E.; Milne, G. W. A.; Barchi, J. J.; Kazanietz, M. G.; Lewin, N. E.; Blumberg, P. M.; Abushanab, E. Conformationally constrained analogs of diacylglycerol. Interaction of gamma-lactones with the phorbol ester receptor of protein-kinase-C. *J. Am. Chem. Soc.* **1992**, *114*, 1059–1070.
- (57) Tripos Inc., 1699 South Hanley Road, St. Louis, MO 63144 (www.tripos.com).
- (58) Halgren, T. A. Merck molecular force field. 1. Basis, form, scope, parameterization, and performance of MMFF94. *J. Comput. Chem.* **1996**, *17*, 490–519.
- (59) Rarey, M.; Kramer, B.; Lengauer, T.; Klebe, G. A fast flexible docking method using an incremental construction algorithm. *J. Mol. Biol.* **1996**, *261*, 470–489.
- (60) Bower, M. J.; Cohen, F. E.; Dunbrack, R. L. Prediction of protein side-chain rotamers from a backbone-dependent rotamer library: a new homology modeling tool. *J. Mol. Biol.* **1997**, *267*, 1268–1282.
- (61) Brooks, B. R.; Brucoleri, R. E.; Olafson, B. D.; States, D. J.; Swaminathan, S.; Karplus, M. Charmm, a program for macromol-

- lecular energy, minimization, and dynamics calculations. *J. Comput. Chem.* **1983**, *4*, 187–217.
- (62) MacKerell, A. D.; Bashford, D.; Bellott, M.; Dunbrack, R. L.; Evanseck, J. D.; Field, M. J.; Fischer, S.; Gao, J.; Guo, H.; Ha, S.; Joseph-McCarthy, D.; Kuchnir, L.; Kuczera, K.; Lau, F. T. K.; Mattos, C.; Michnick, S.; Ngo, T.; Nguyen, D. T.; Prodhom, B.; Reiher, W. E.; Roux, B.; Schlenkrich, M.; Smith, J. C.; Stote, R.; Straub, J.; Watanabe, M.; Wiorkiewicz-Kuczera, J.; Yin, D.; Karplus, M. All-atom empirical potential for molecular modeling and dynamics studies of proteins. *J. Phys. Chem. B* **1998**, *102*, 3586–3616.
- (63) Mackerell, A. D.; Feig, M.; Brooks, C. L. Extending the treatment of backbone energetics in protein force fields: limitations of gas-phase quantum mechanics in reproducing protein conformational distributions in molecular dynamics simulations. *J. Comput. Chem.* **2004**, *25*, 1400–1415.
- (64) Nina, M.; Beglov, D.; Roux, B. Atomic radii for continuum electrostatics calculations based on molecular dynamics free energy simulations. *J. Phys. Chem. B* **1997**, *101*, 5239–5248.

JM0702579